

# Towards the deployment of DAMIC-M: status and latest results



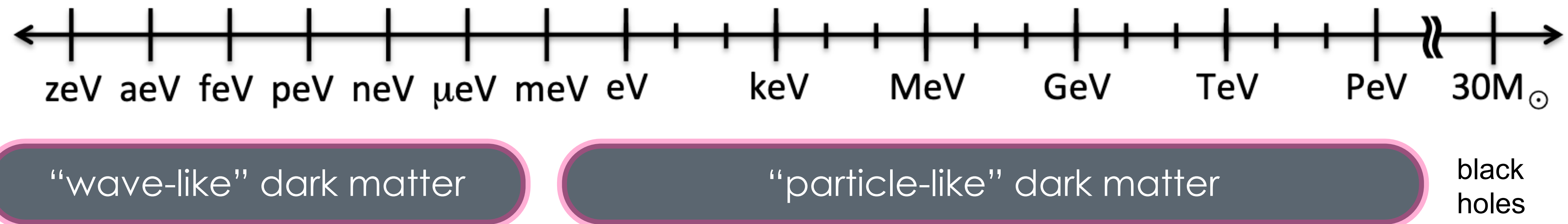
*Michelangelo Traina, on behalf of the DAMIC-M collaboration*  
Instituto de Física de Cantabria (IFCA), Santander, Spain

## Outline:

1. Dark Matter
2. Scientific CCDs
3. DAMIC-M and LBC
4. Latest Science Results
5. Status and Prospects
6. Conclusions



# Dark Matter... and where to find it

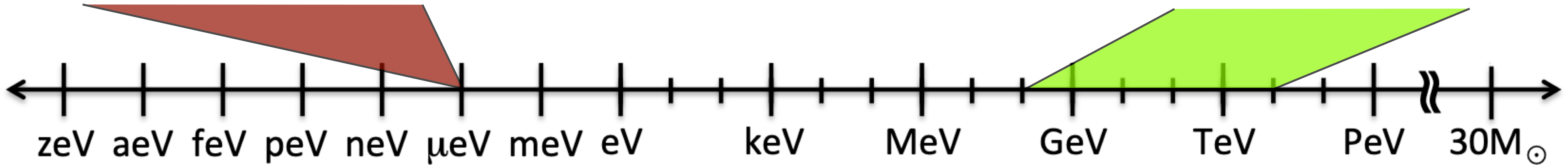
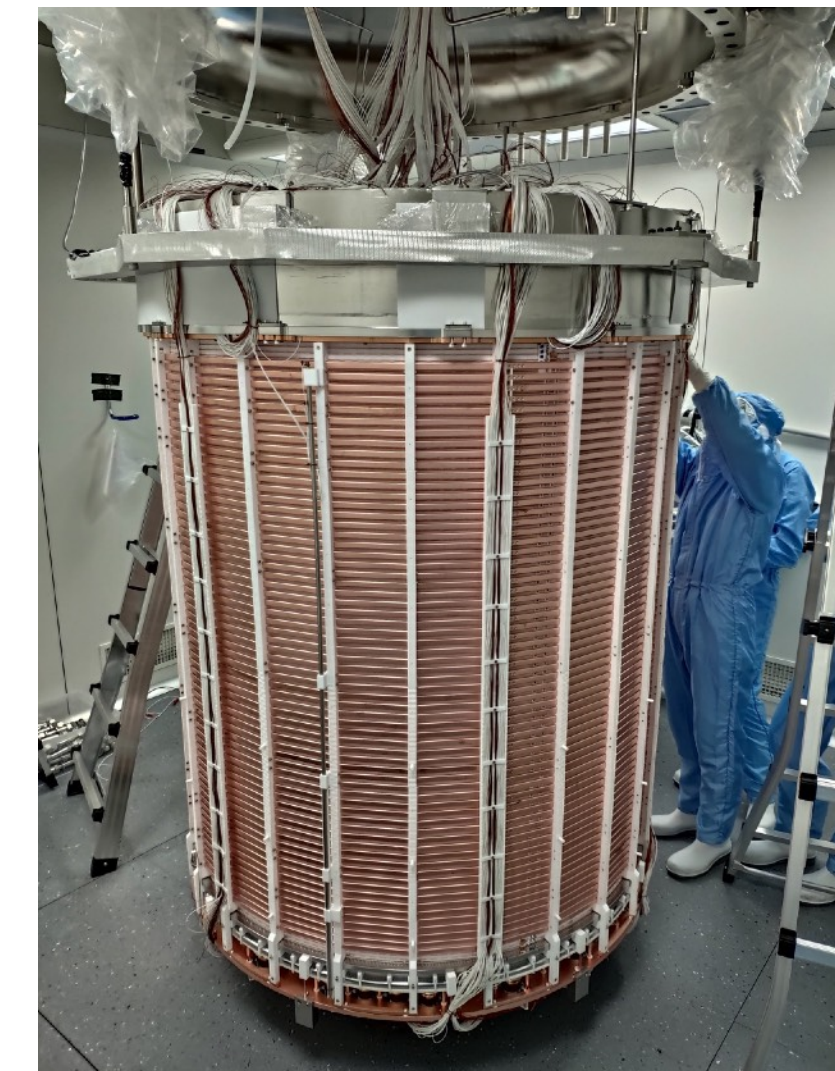


# Dark Matter... and how to find it

ADMX



XENON



“wave-like” dark matter

“particle-like” dark matter

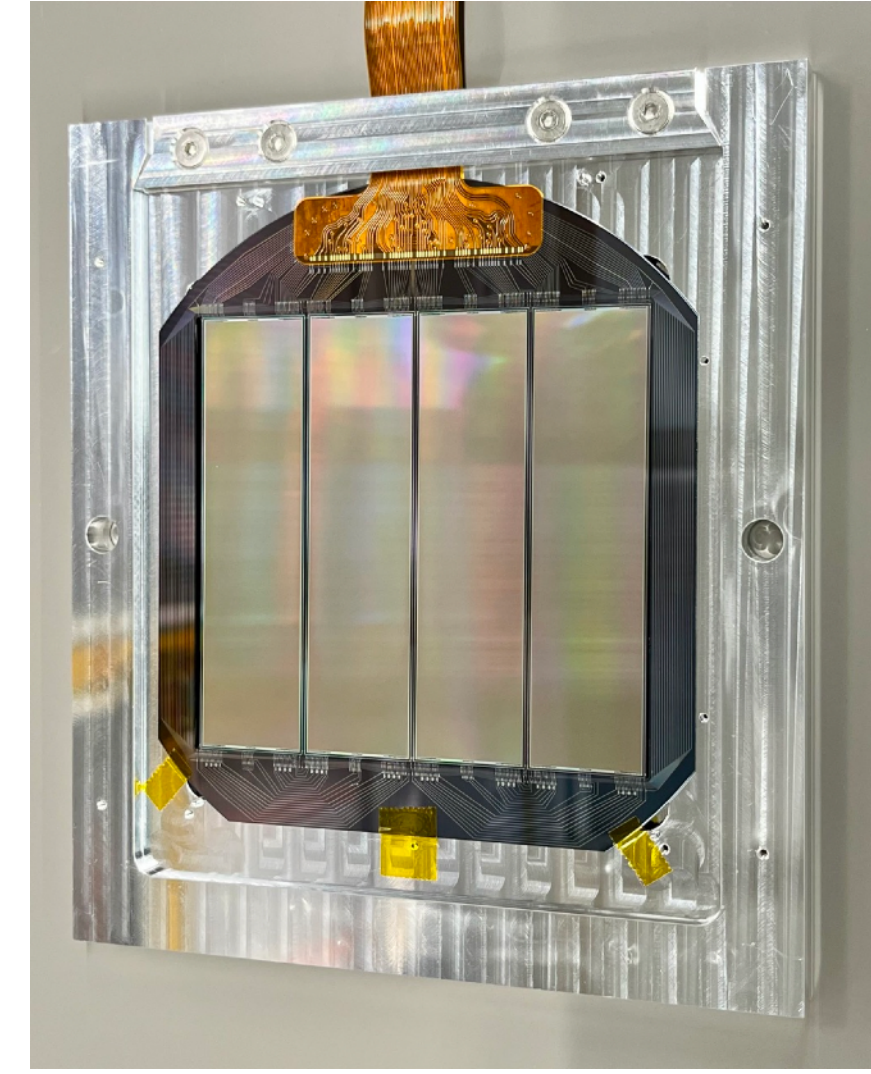
black  
holes

# Dark Matter... and how to find it

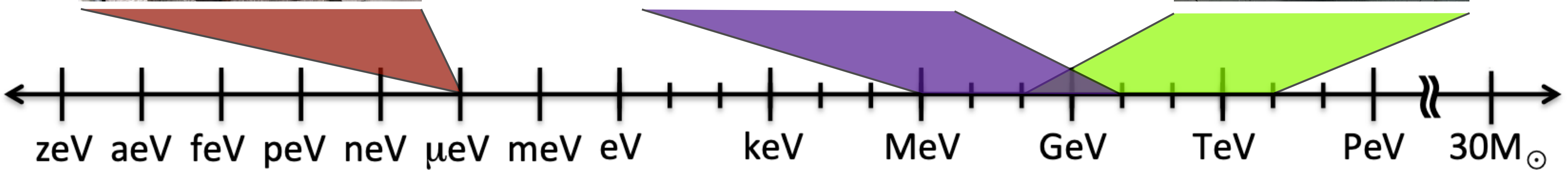
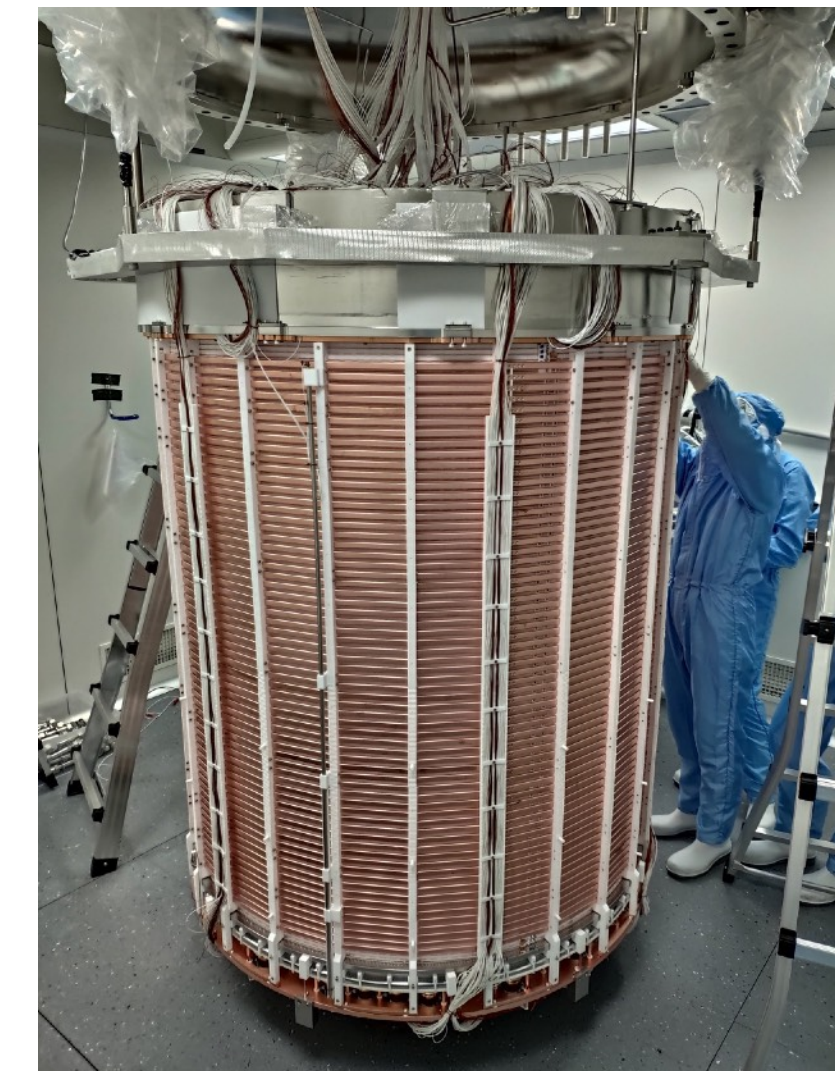
ADMX



DAMIC-M



XENON



“wave-like” dark matter

“particle-like” dark matter

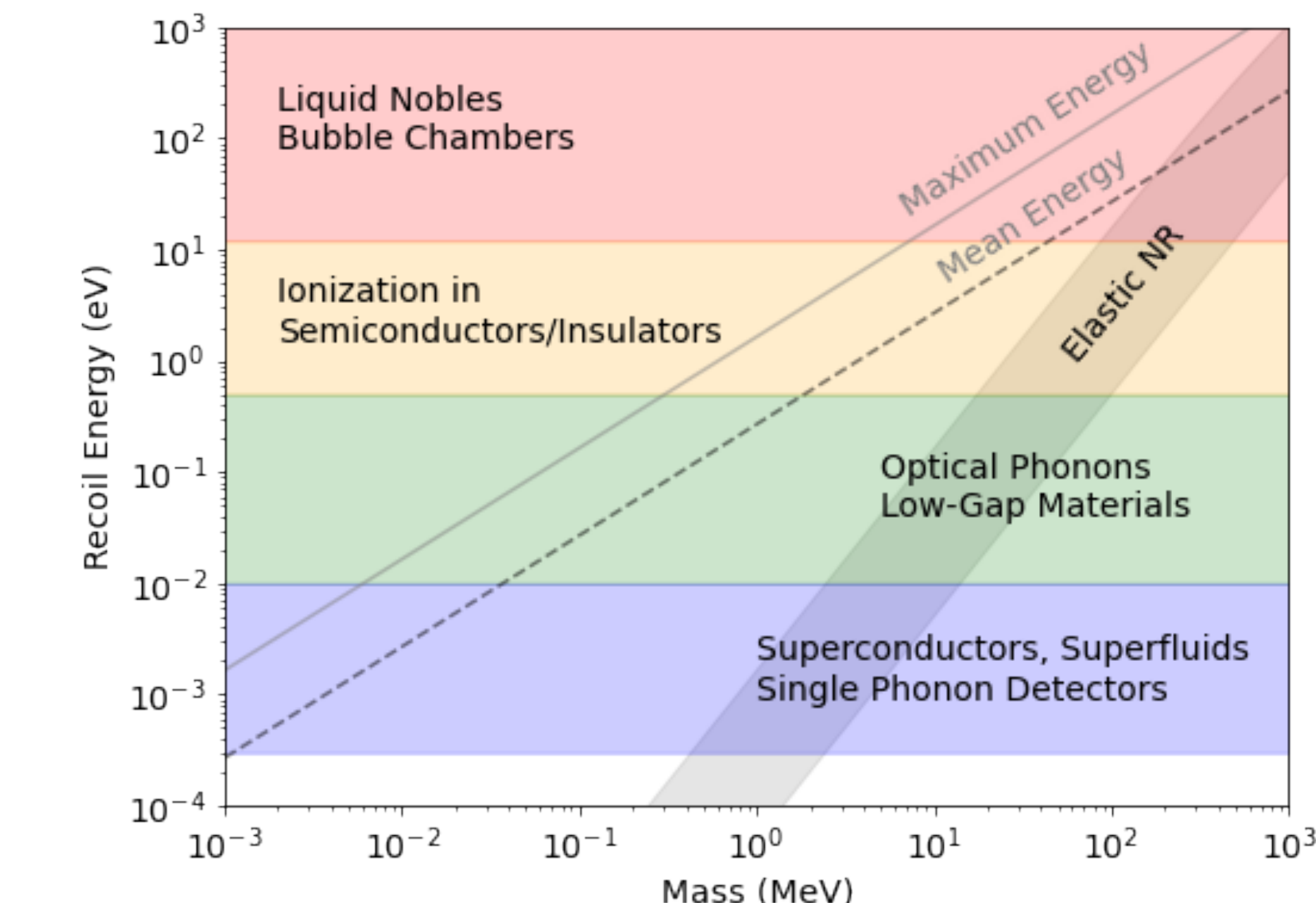
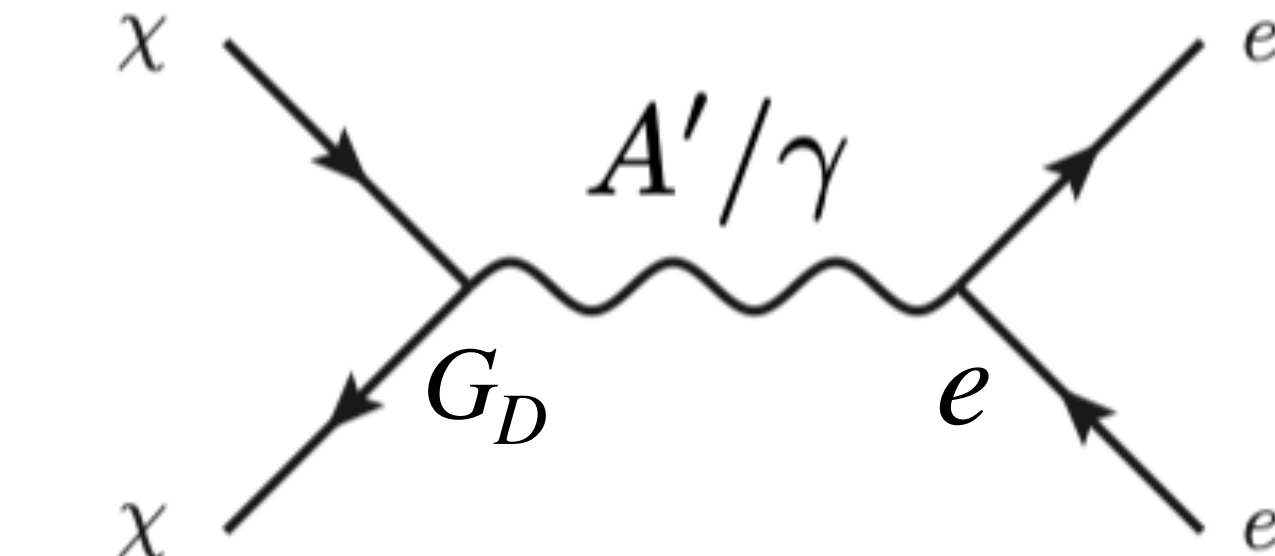
black  
holes



# DM-e<sup>-</sup> scattering

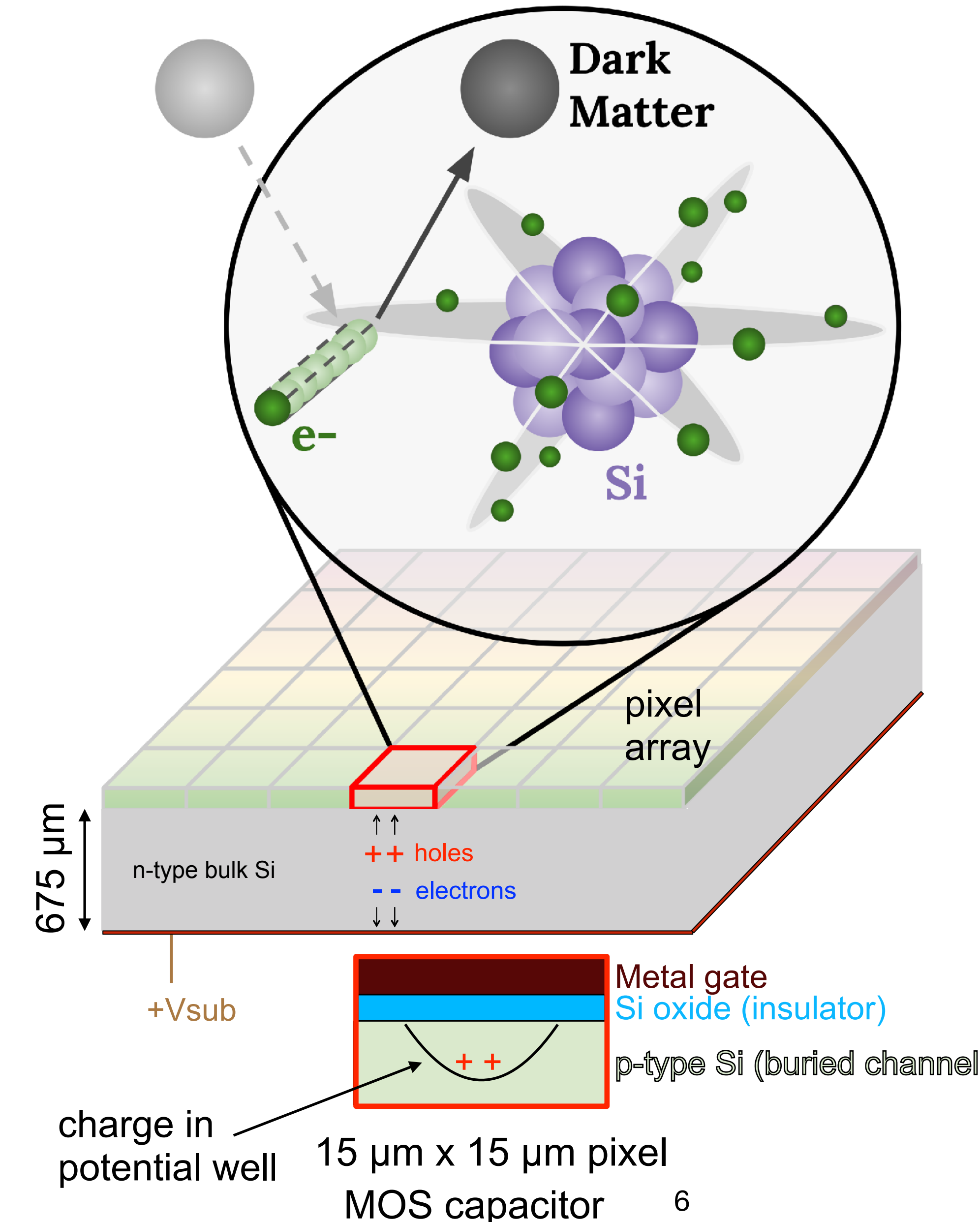
- WIMP miracle: weak-scale coupling and mass. WIMPs undetected so far.
- WIMPless miracle: new couplings and mass scales in the hidden sector.
  - Simple mechanism: DM-e<sup>-</sup> through a massive mediator mixed with the photon.  
→ Probe DM via electronic recoil.
  - Electrons are a lighter target and offer full ionization yield. However:
    - DM  $\vec{Q}$  must overlap with crystal response.
    - No coherent enhancement, unlike DM-n scatter.

$$\Omega_X \sim \langle \sigma_A v \rangle^{-1} \sim \frac{m_X^2}{g_X^4}$$



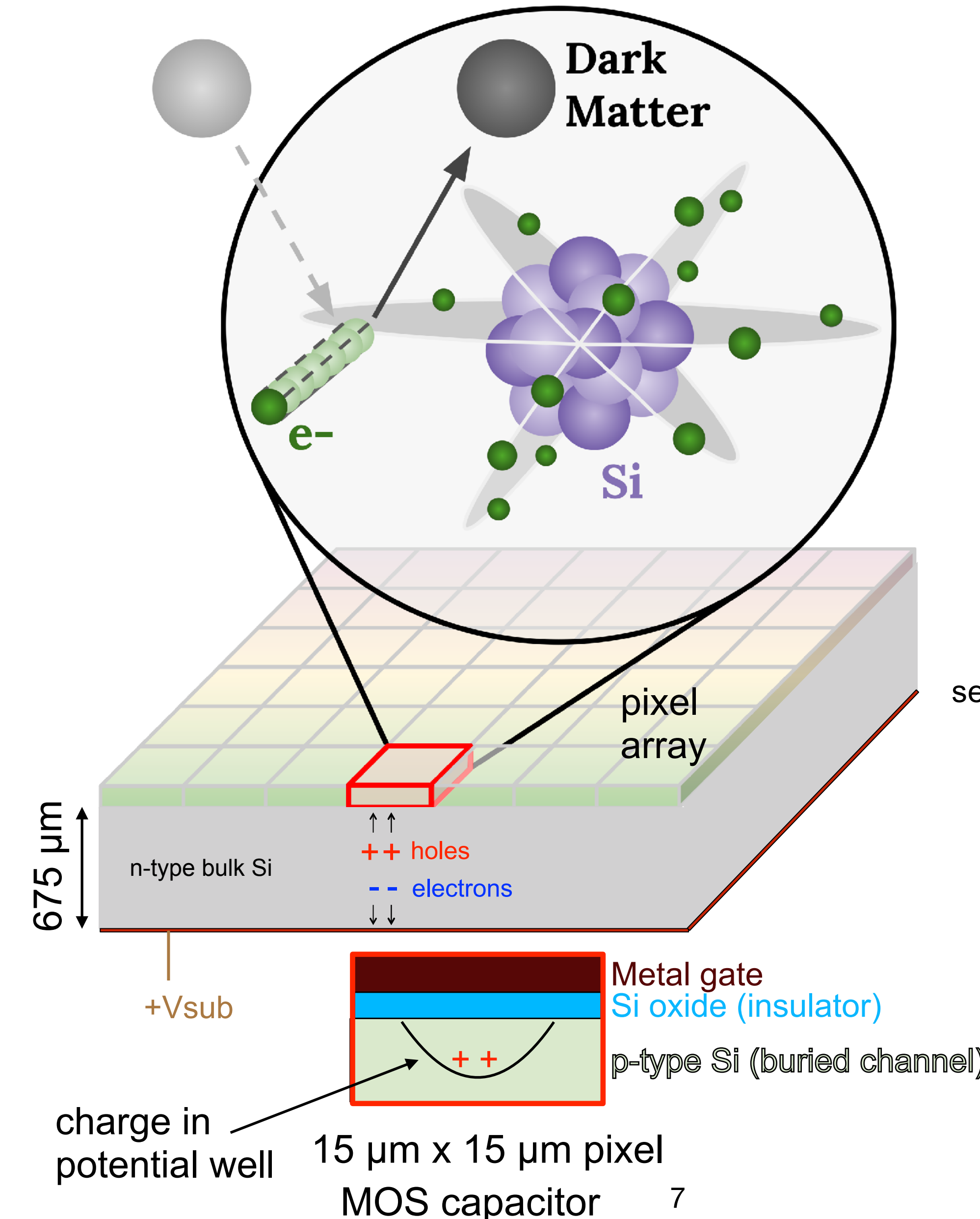
# Scientific CCDs

- P-type buried channel structure (LBNL).
- Fully depleted at 40 V ( $\sim 10 \text{ k}\Omega \cdot \text{cm}$ ).
- $15 \mu\text{m} \times 15 \mu\text{m}$  pixel.

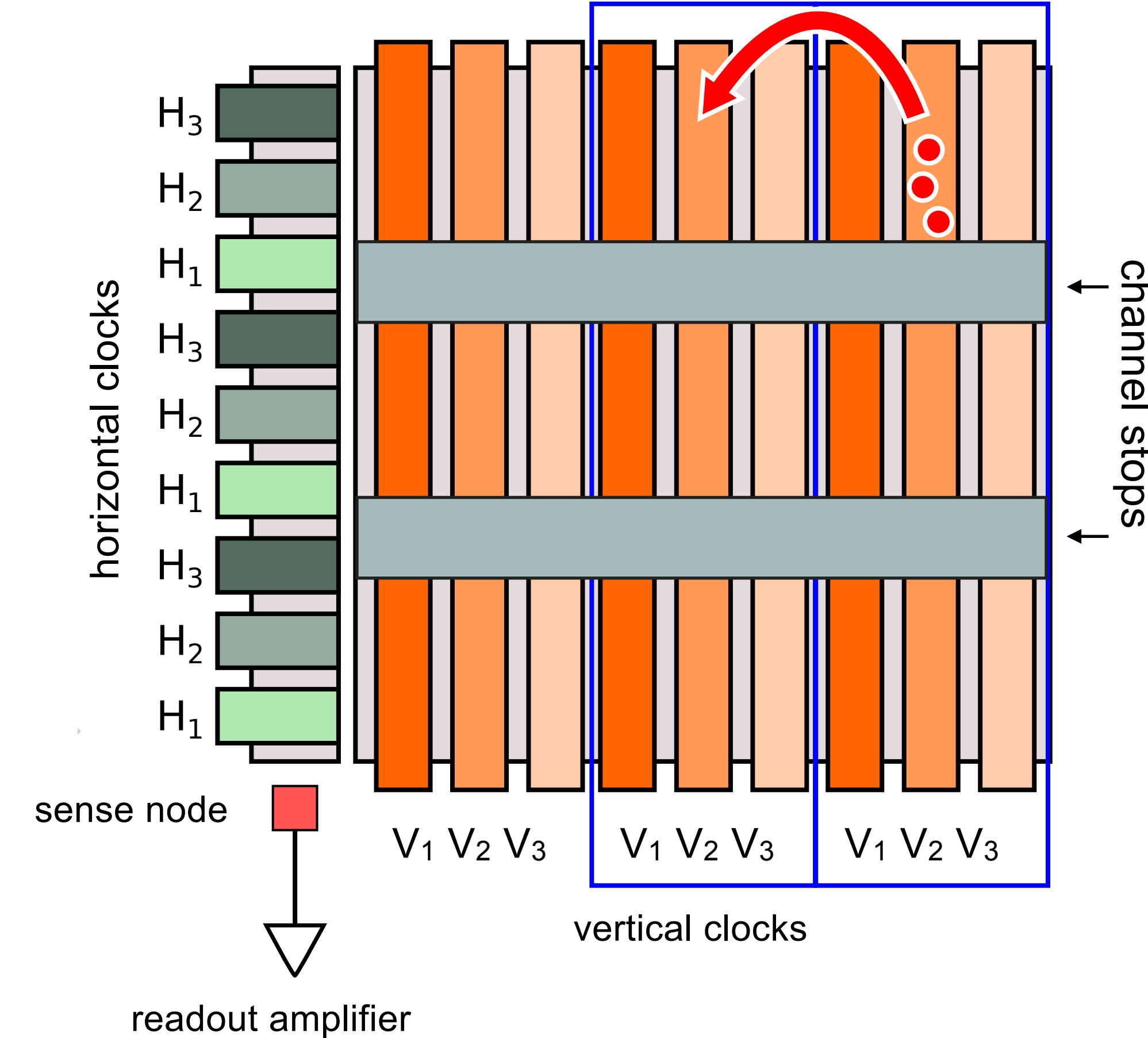


# Scientific CCDs

- P-type buried channel structure (LBNL).
- Fully depleted at 40 V ( $\sim 10 \text{ k}\Omega \cdot \text{cm}$ ).
- $15 \mu\text{m} \times 15 \mu\text{m}$  pixel.
- Charge transfer inefficiency:  $< 10^{-6}$ .
- Readout noise:  $\sim 2 e^-$  (6 eV).

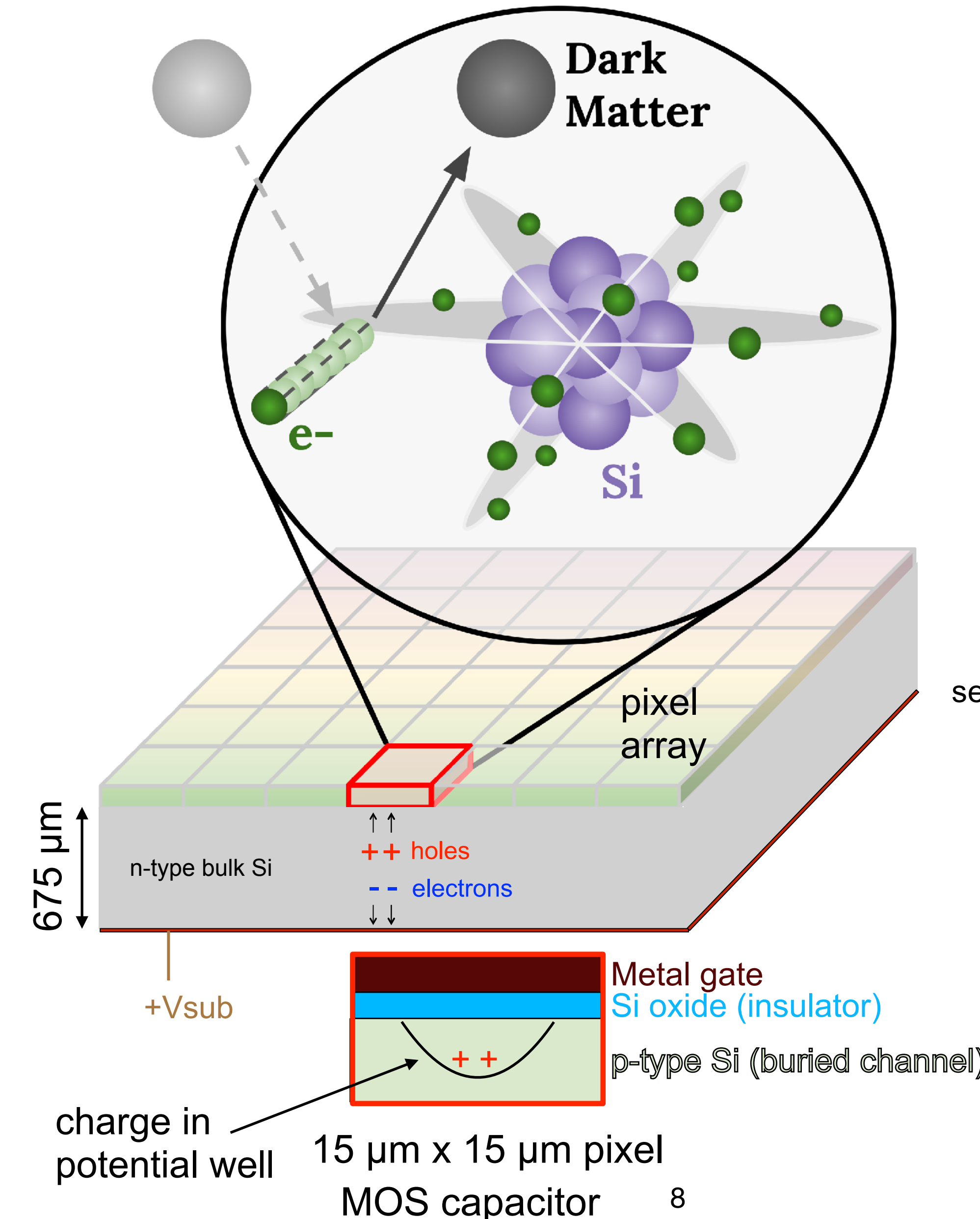


3x3 pixels CCD

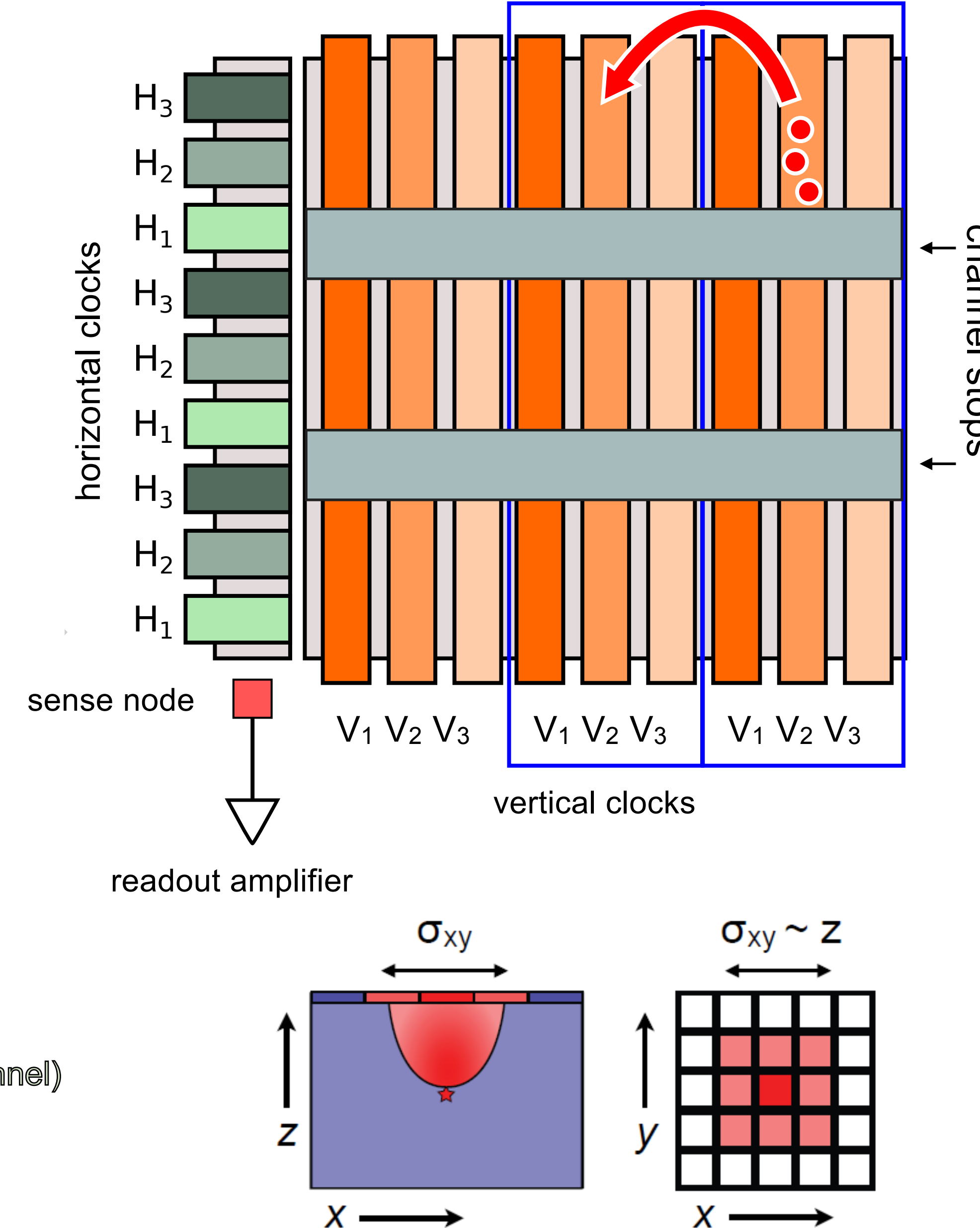


# Scientific CCDs

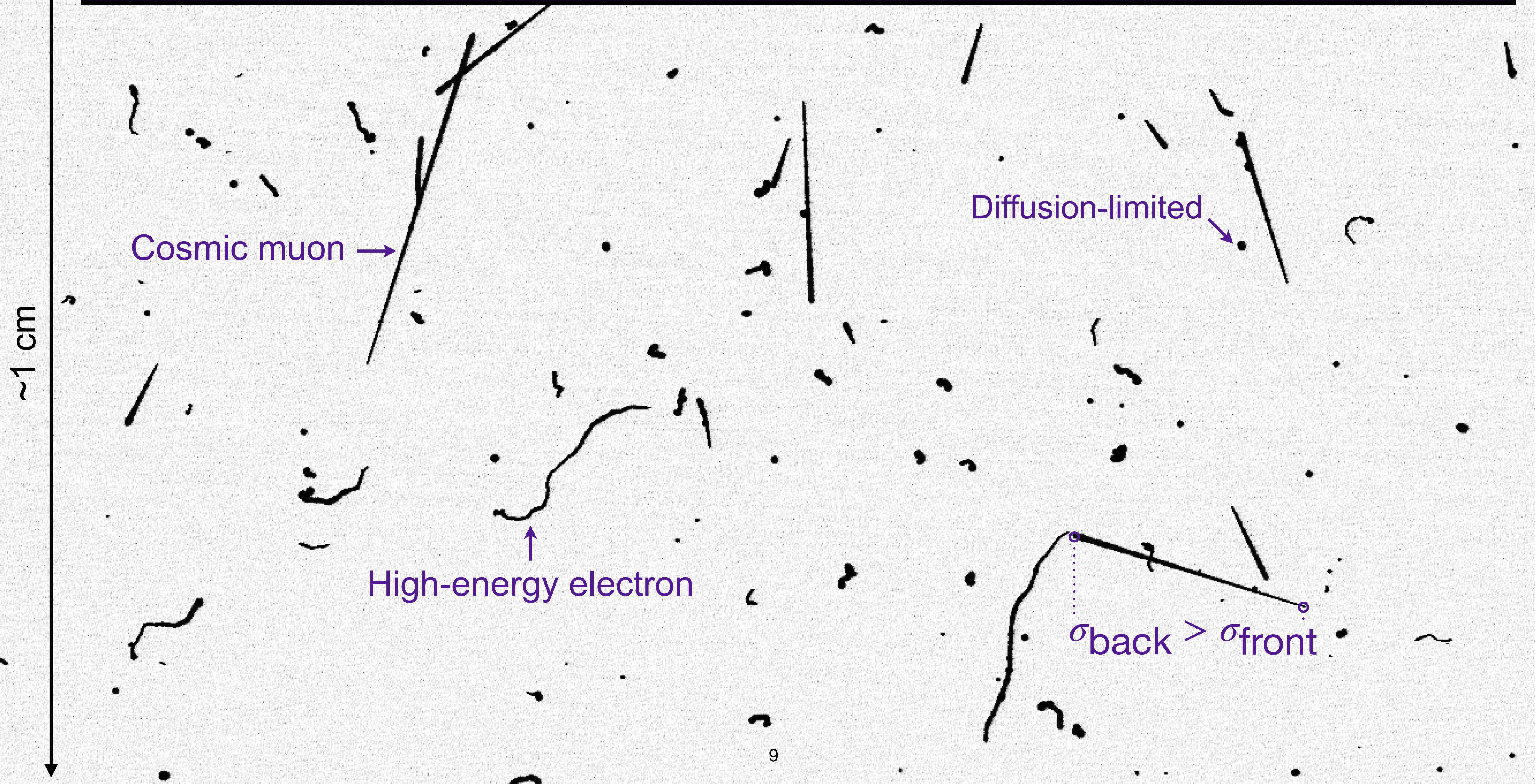
- P-type buried channel structure (LBNL).
- Fully depleted at 40 V ( $\sim 10 \text{ k}\Omega \cdot \text{cm}$ ).
- $15 \mu\text{m} \times 15 \mu\text{m}$  pixel.
- Charge transfer inefficiency:  $< 10^{-6}$ .
- Readout noise:  $\sim 2 e^-$  (6 eV).
- Depth (z) reconstructed from distribution of charge on pixel array.



3x3 pixels CCD

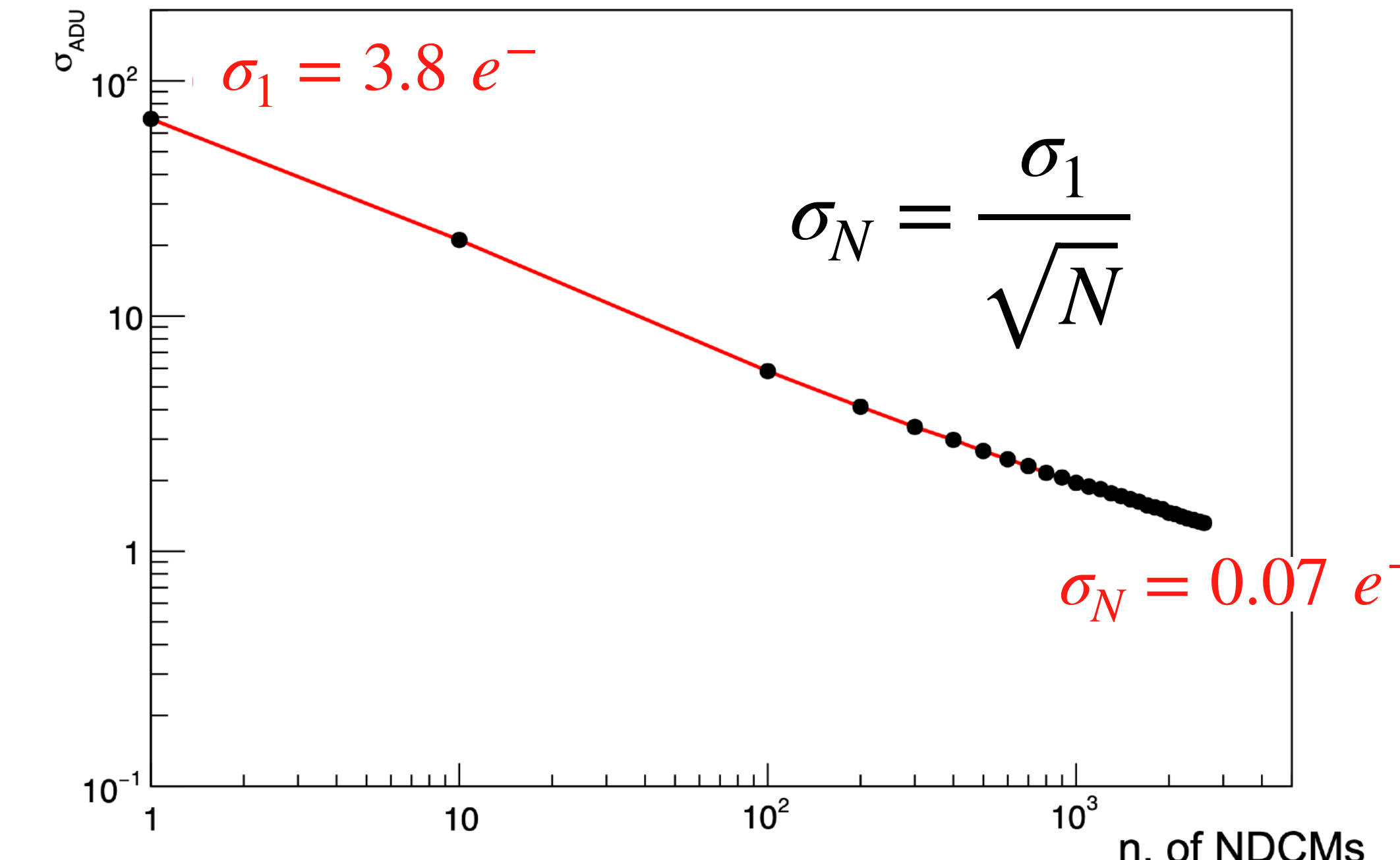
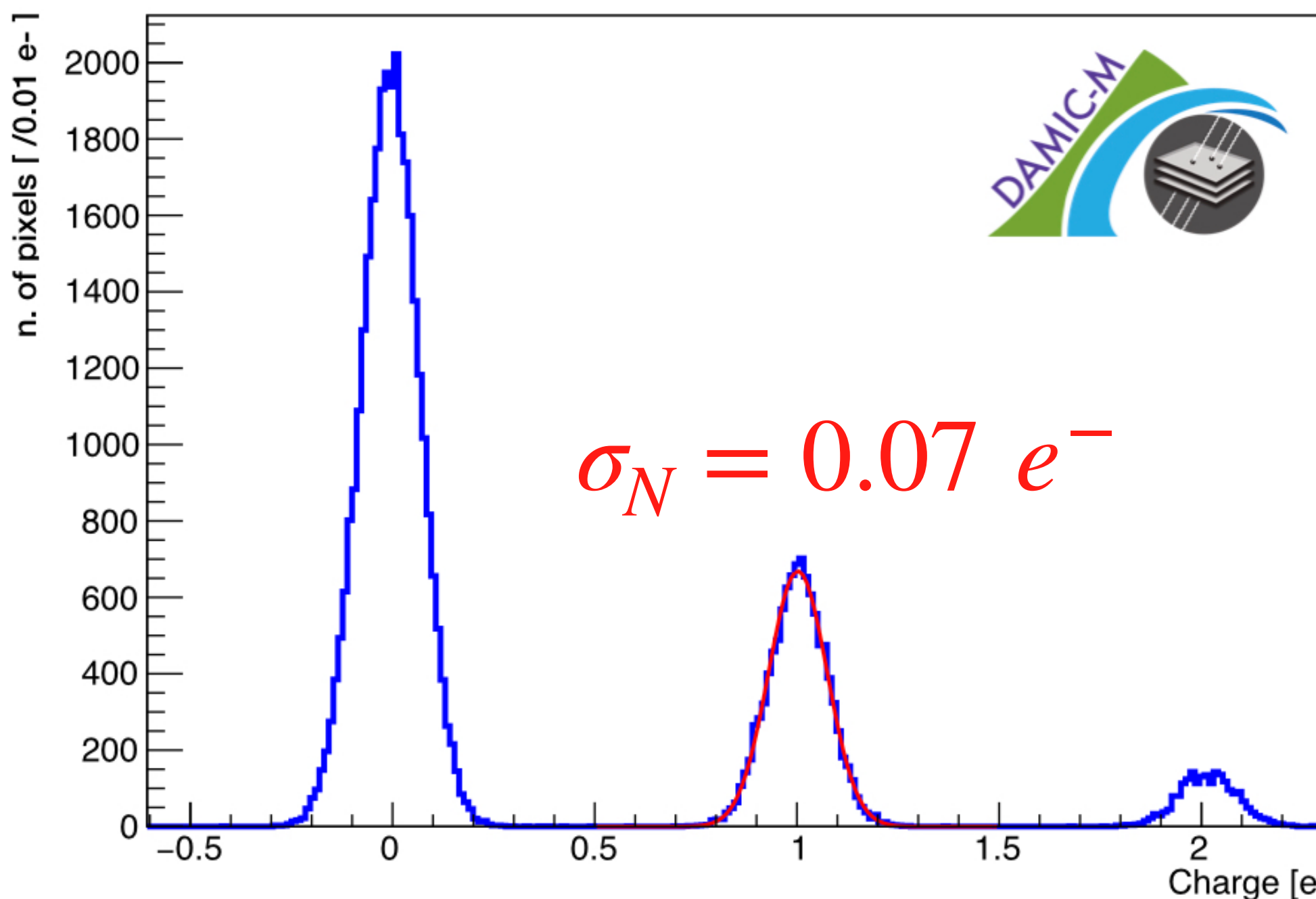
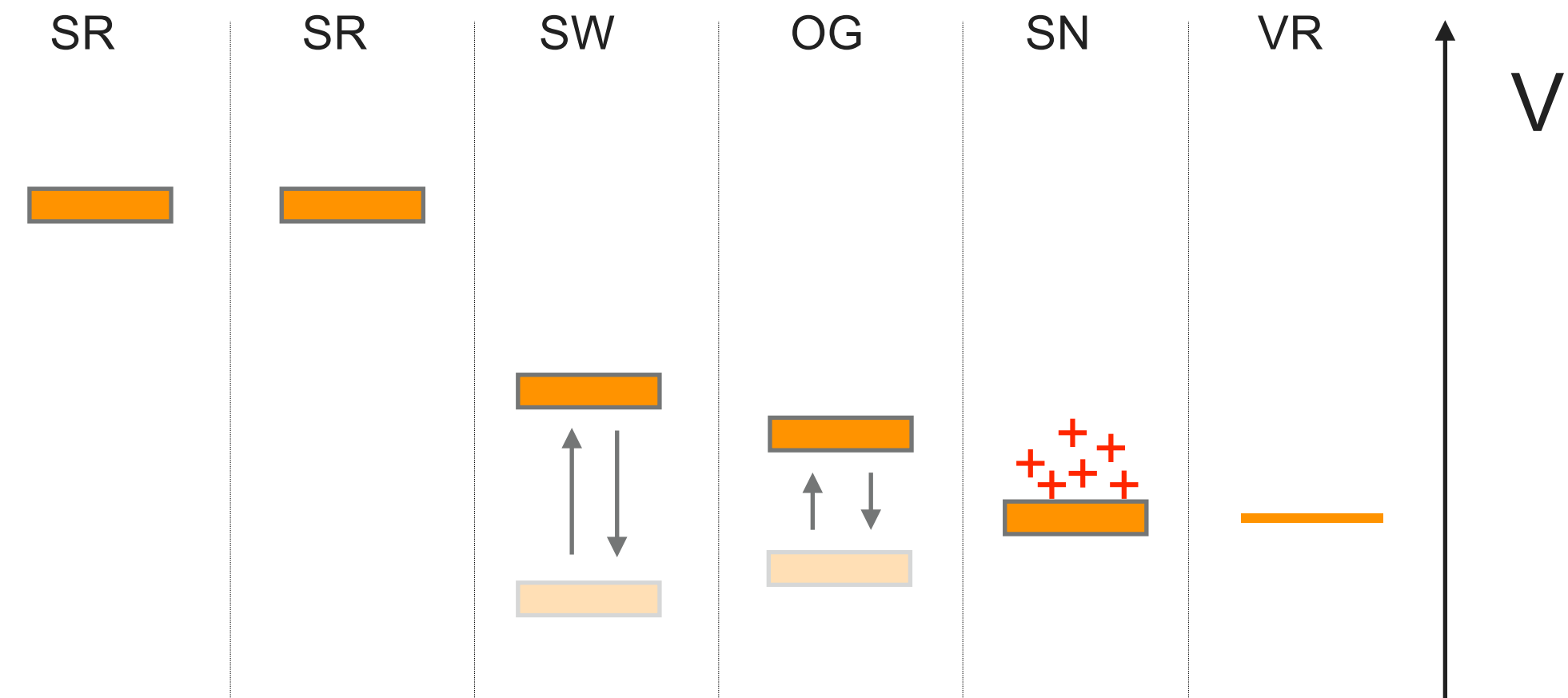


# Sample CCD image in the surface lab (~15 min exposure).

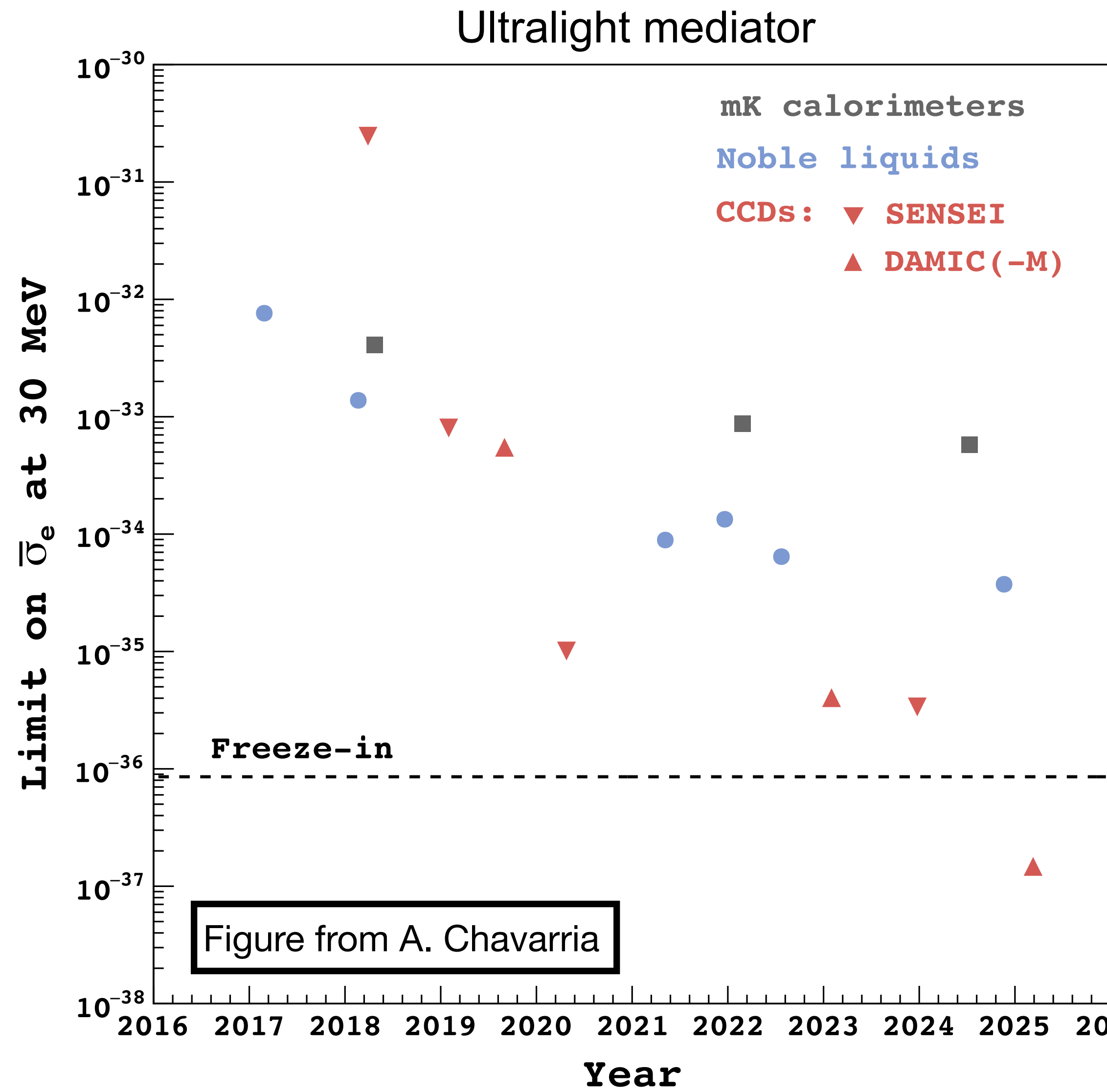


# Skipper readout

- Non-destructive charge measurement (Janesick et al. 1990).
- Re-engineered for LBNL CCDs (Tiffenberg et al. 2017).
- Sub-electron resolution via NDCMs.



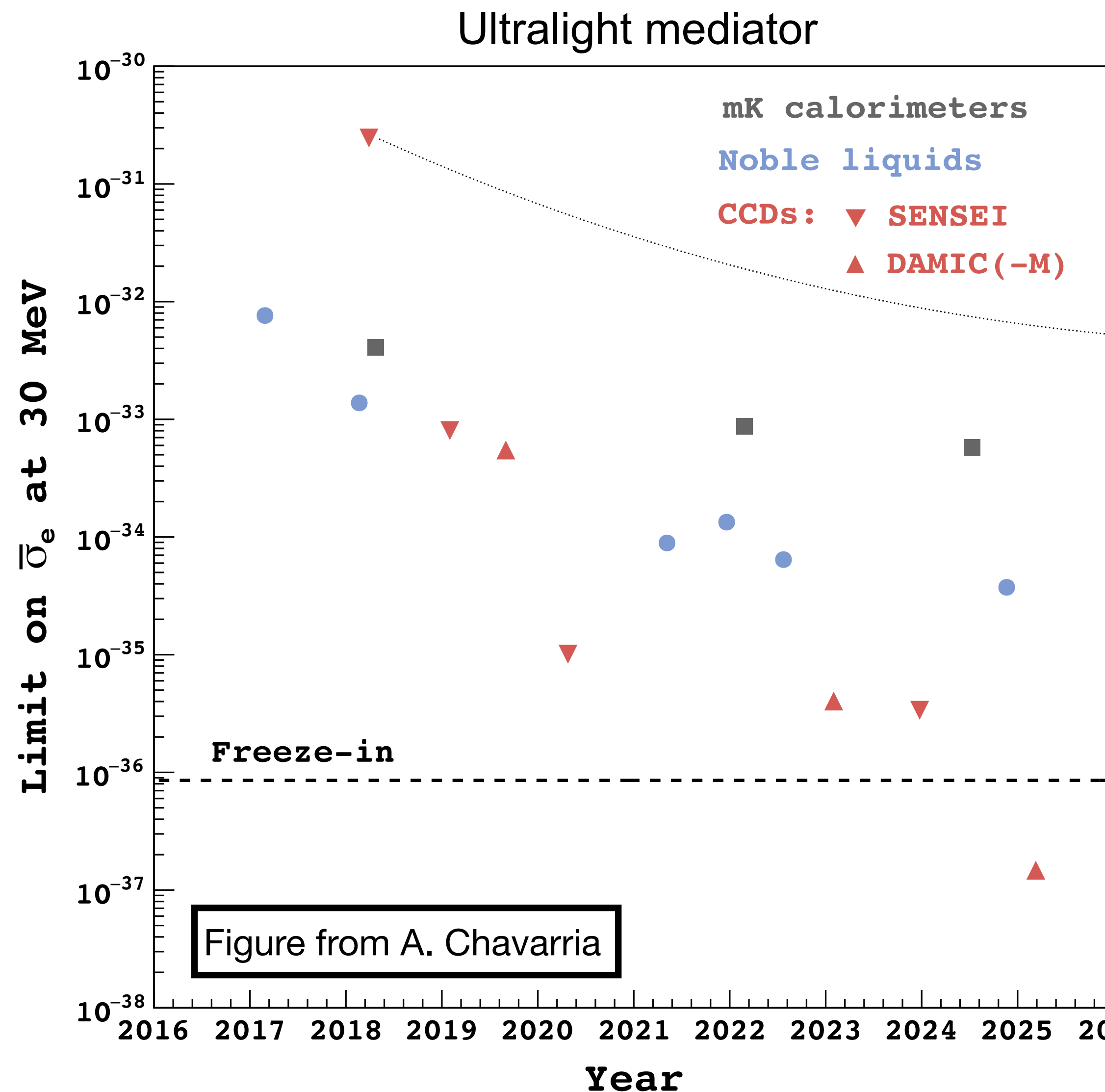
# DArk Matter In CCDs: Timeline



2012: DAMIC at SNOLAB starts: first low-bkg CCD array for DM searches.



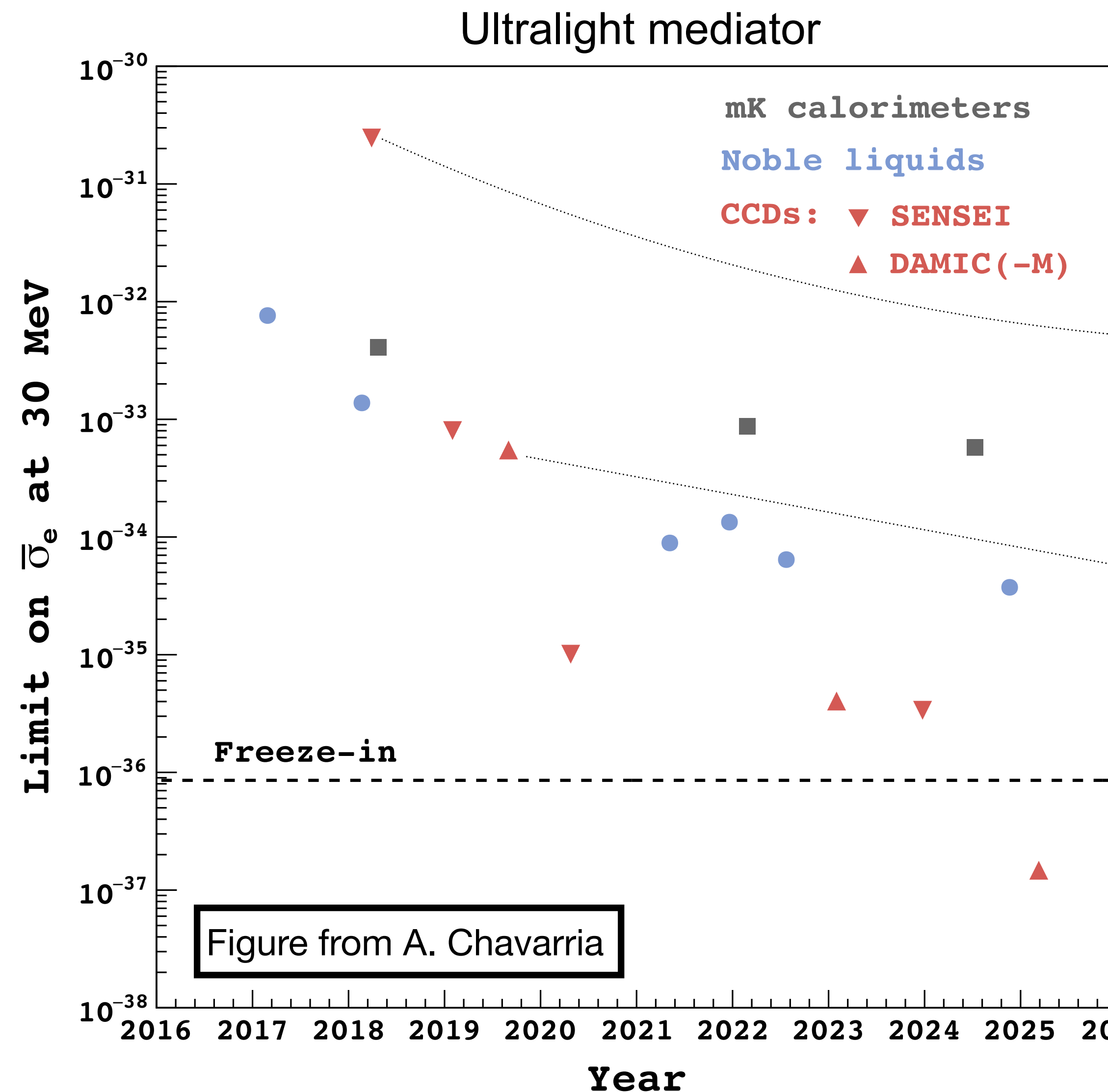
# DArk Matter In CCDs: Timeline



2012: DAMIC at SNOLAB starts: first low-bkg CCD array for DM searches.

2017: Two skipper-CCD experiments start: SENSEI and DAMIC-M.

# DArk Matter In CCDs: Timeline

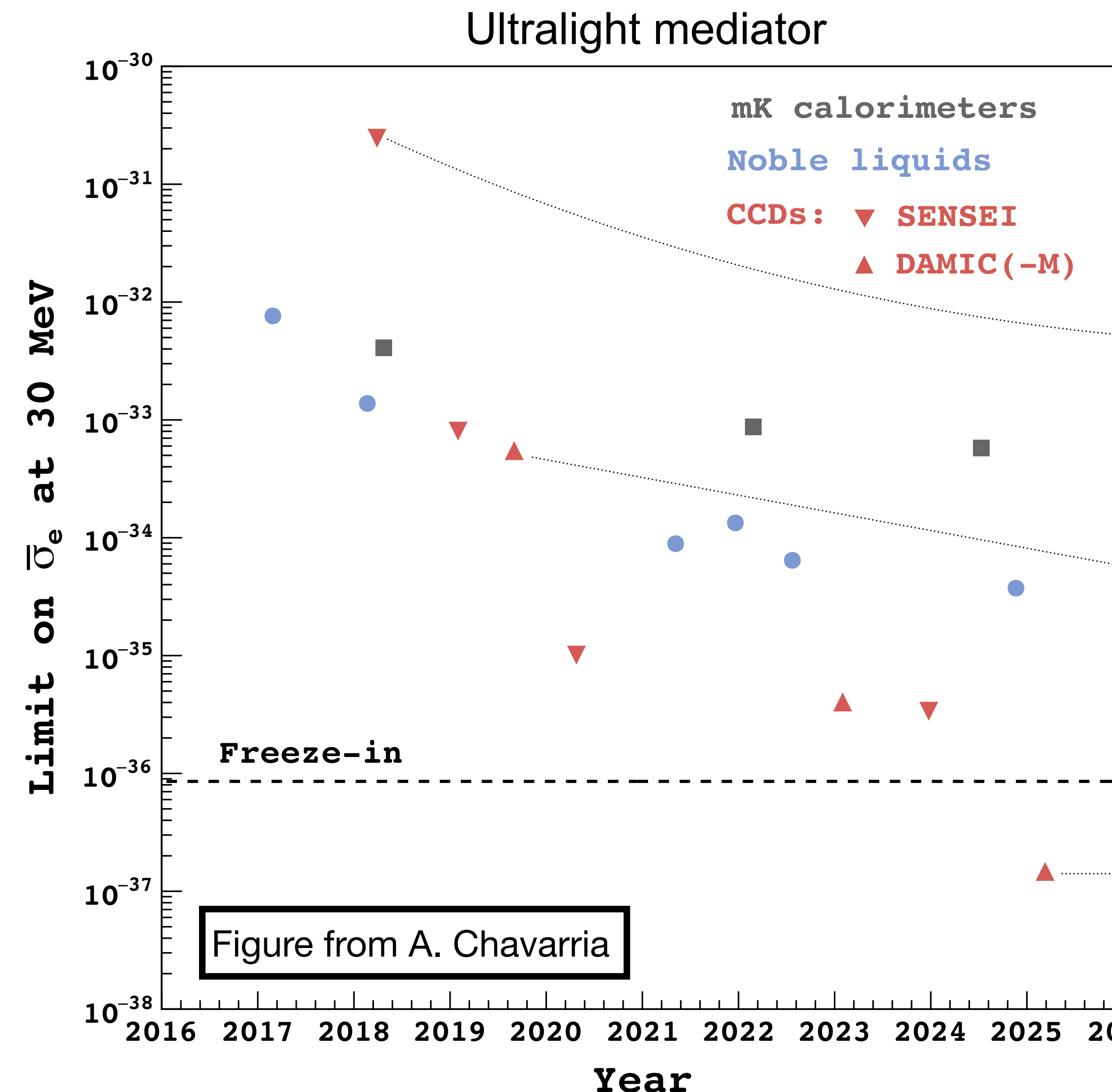


2012: DAMIC at SNOLAB starts: first low-bkg CCD array for DM searches.

2017: Two skipper-CCD experiments start: SENSEI and DAMIC-M.

2019: DAMIC at SNOLAB publish first  $DMe^-$  results.

# DArk Matter In CCDs: Timeline



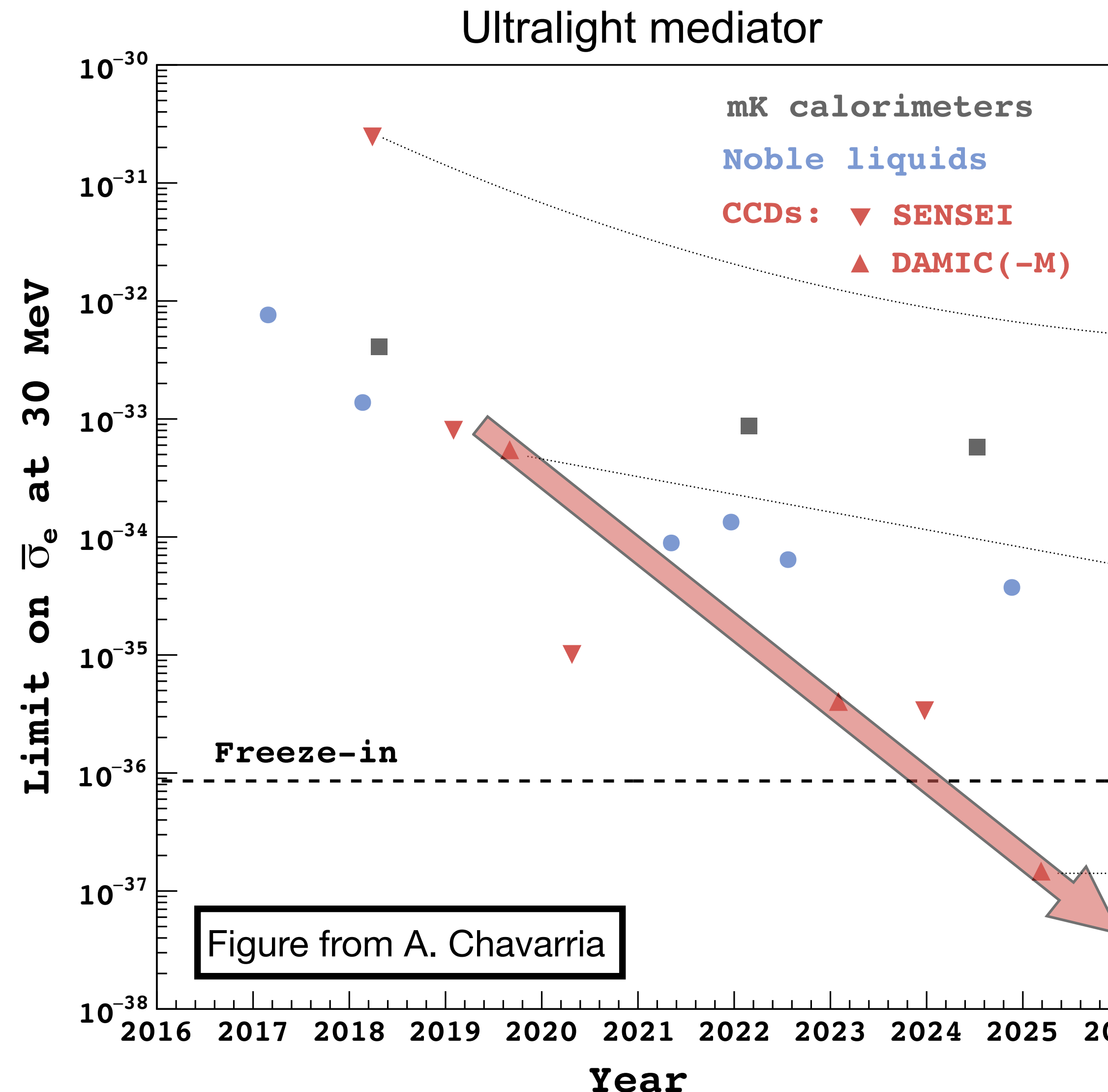
2012: DAMIC at SNOLAB starts: first low-bkg CCD array for DM searches.

2017: Two skipper-CCD experiments start: SENSEI and DAMIC-M.

2019: DAMIC at SNOLAB publish first  $DMe^-$  results.

2025: DAMIC-M's LBC probes benchmark hidden-sector models!

# DArk Matter In CCDs: Timeline



2012: DAMIC at SNOLAB starts: first low-bkg CCD array for DM searches.

2017: Two skipper-CCD experiments start: SENSEI and DAMIC-M.

2019: DAMIC at SNOLAB publish first  $DMe^-$  results.

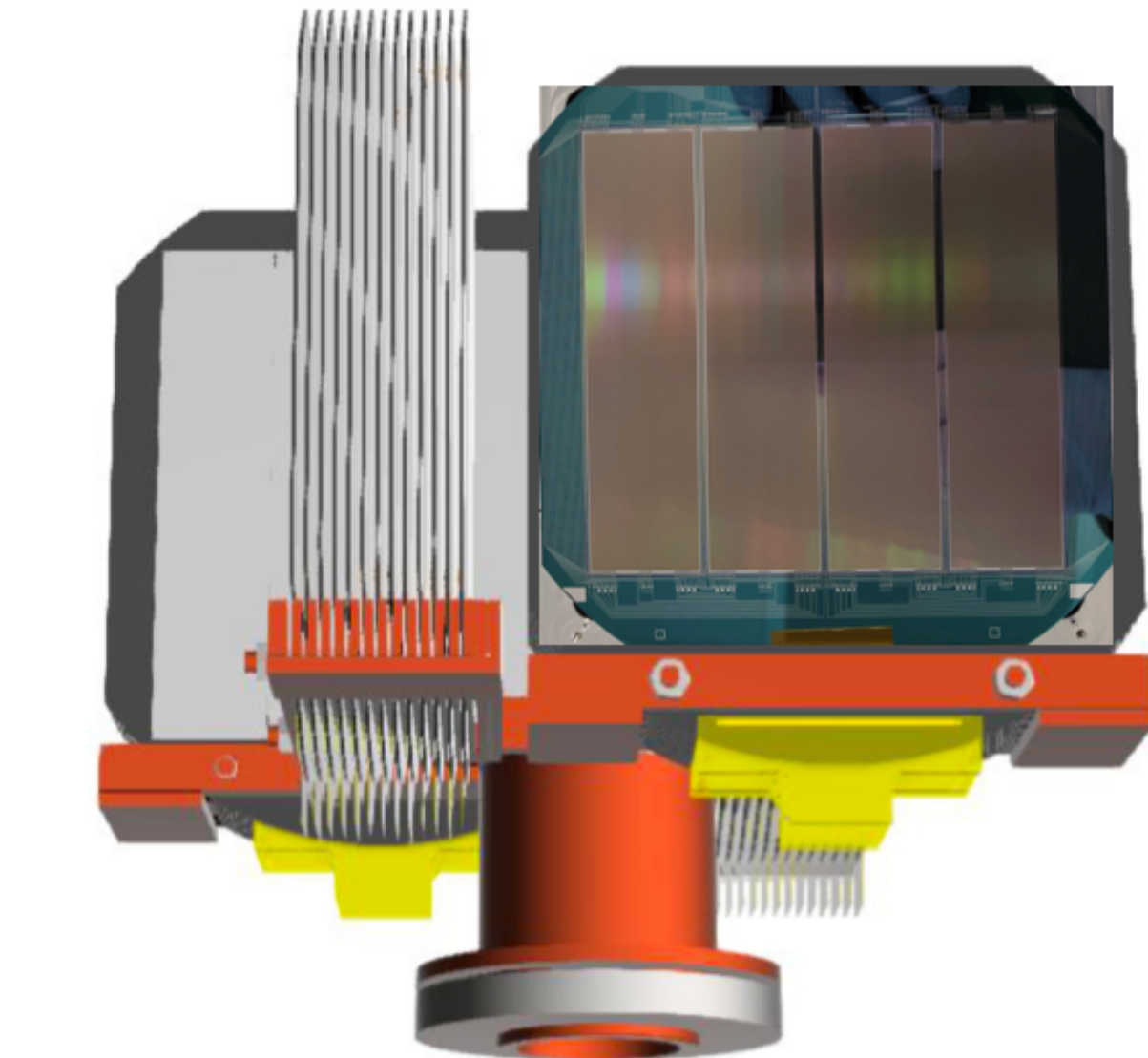
2025: DAMIC-M's LBC probes benchmark hidden-sector models!

# The DAMIC-M Experiment

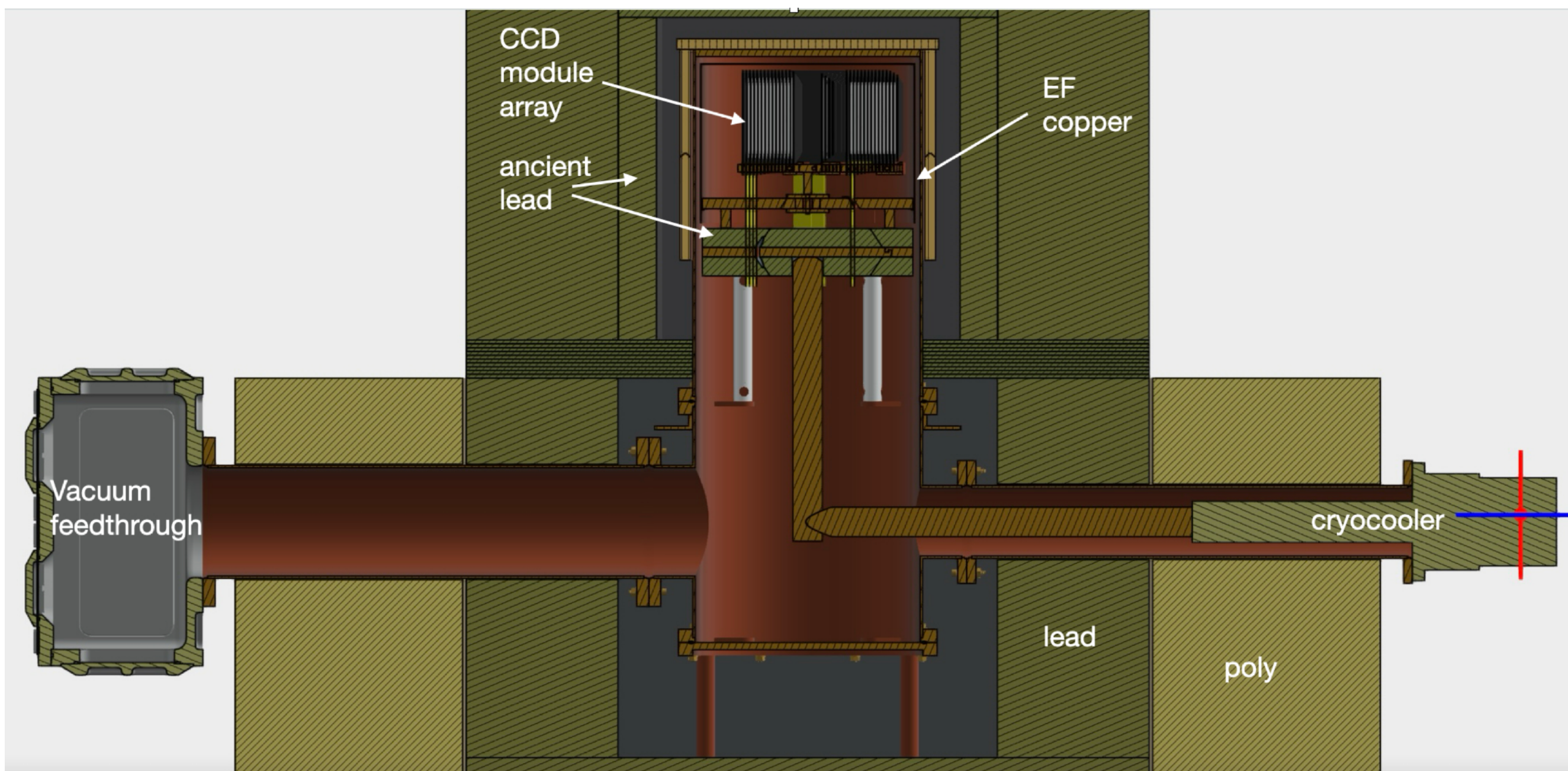
- 52 CCD modules in LSM (France) for kg-year target exposures ( $\sim 700$  g sensitive mass).
- Skipper readout for sensitivity to single charges.
- Background below 1 d.r.u. (events per keV-kg-day).
- Installation early 2026!

DAMIC-M: DArk Matter In CCDs at Modane

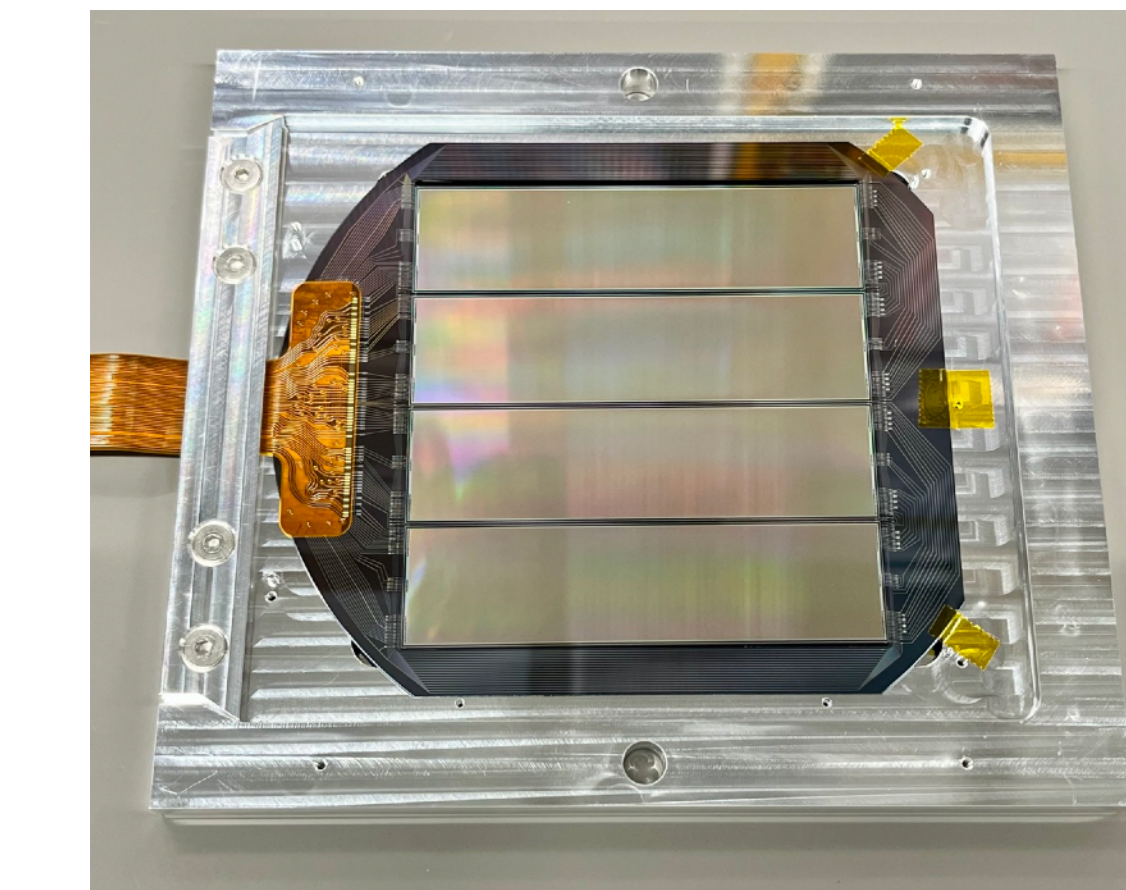
25 cm



Rendering of DAMIC-M CCD array



Rendering of DAMIC-M final design



DAMIC-M CCD module

# The Low-Background Chamber

- Low-background DAMIC-M prototype (~7 dru). Operational since 2021.
- Objectives: CCD performance, backgrounds, components for DAMIC-M, and first science results with skipper CCDs.
- World-leading results in 2023, 2024 and 2025.

PRL130(2023)171003

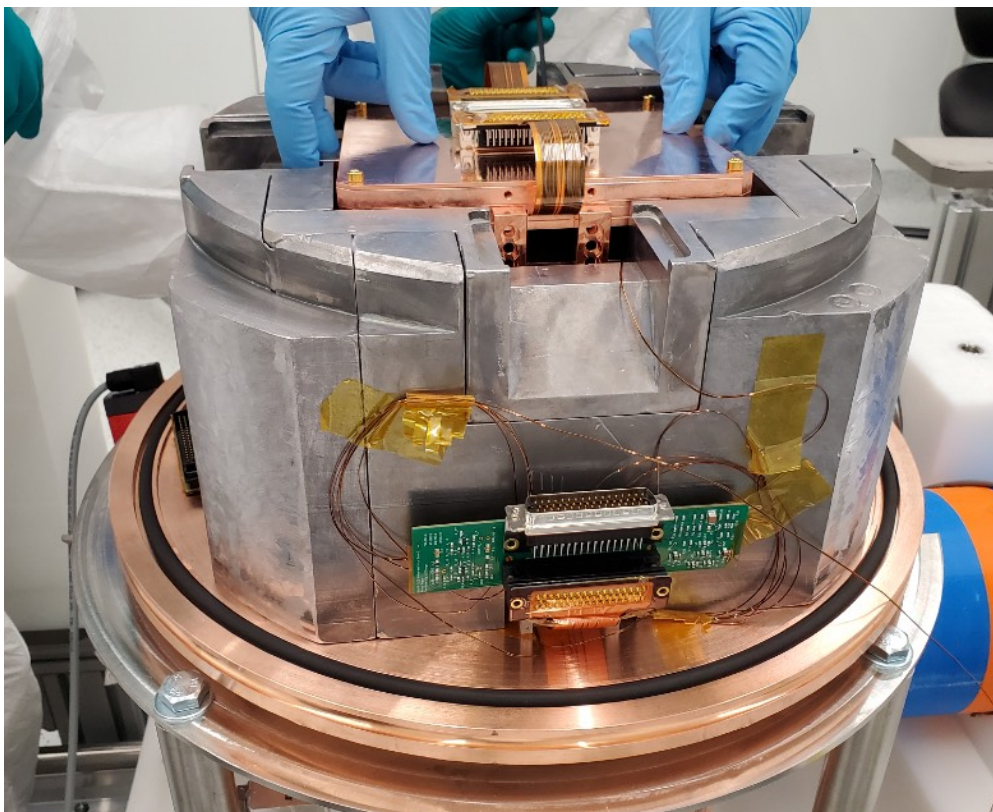
PRL132(2024)101006

PRL135(2025)071002

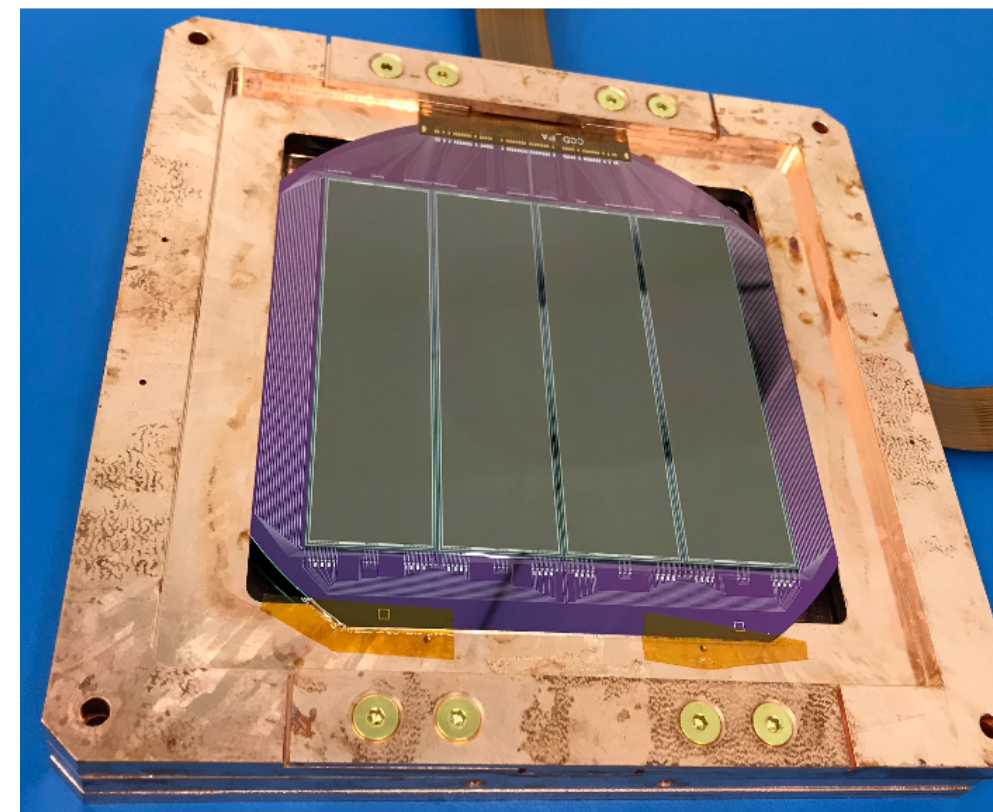
SR1 (science run 1)

SR1

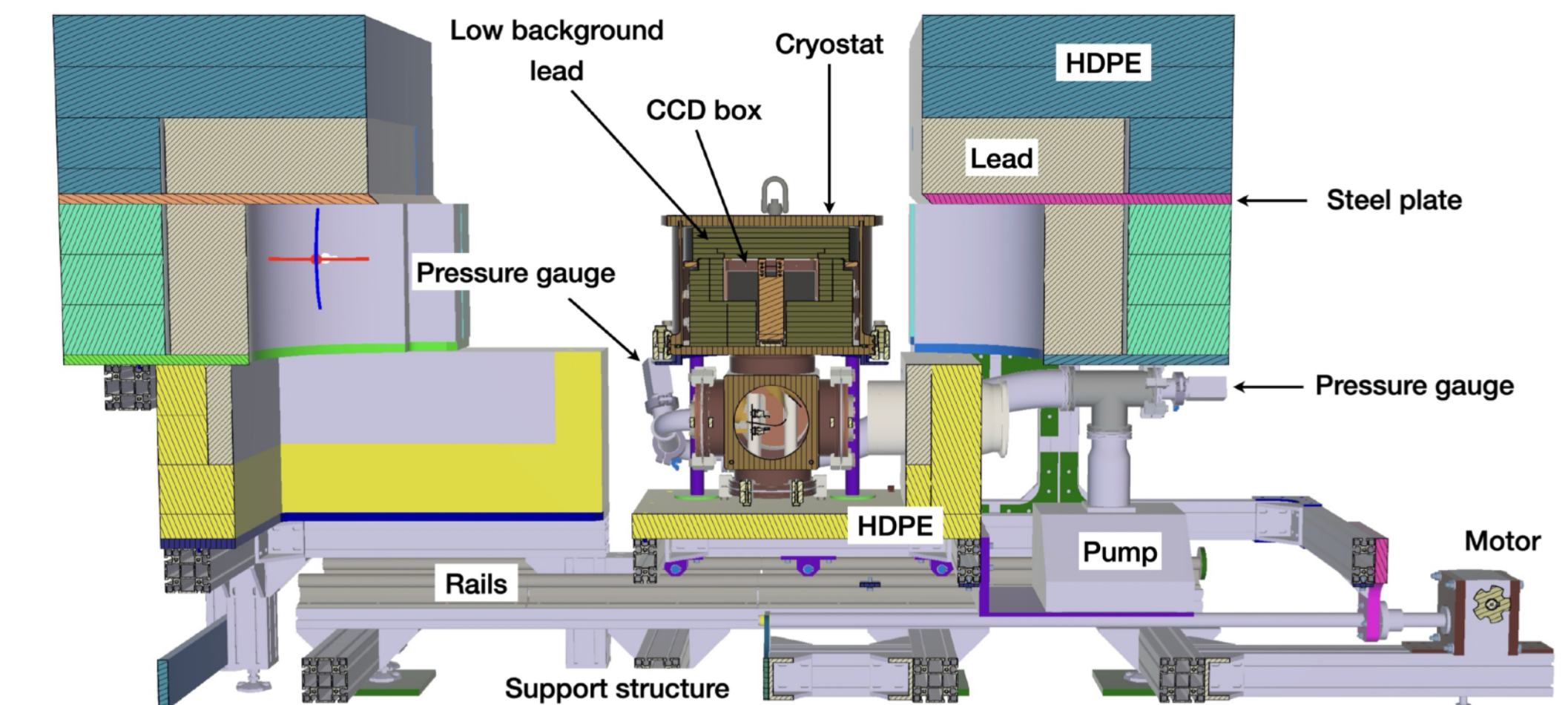
SR2



Inner cryostat

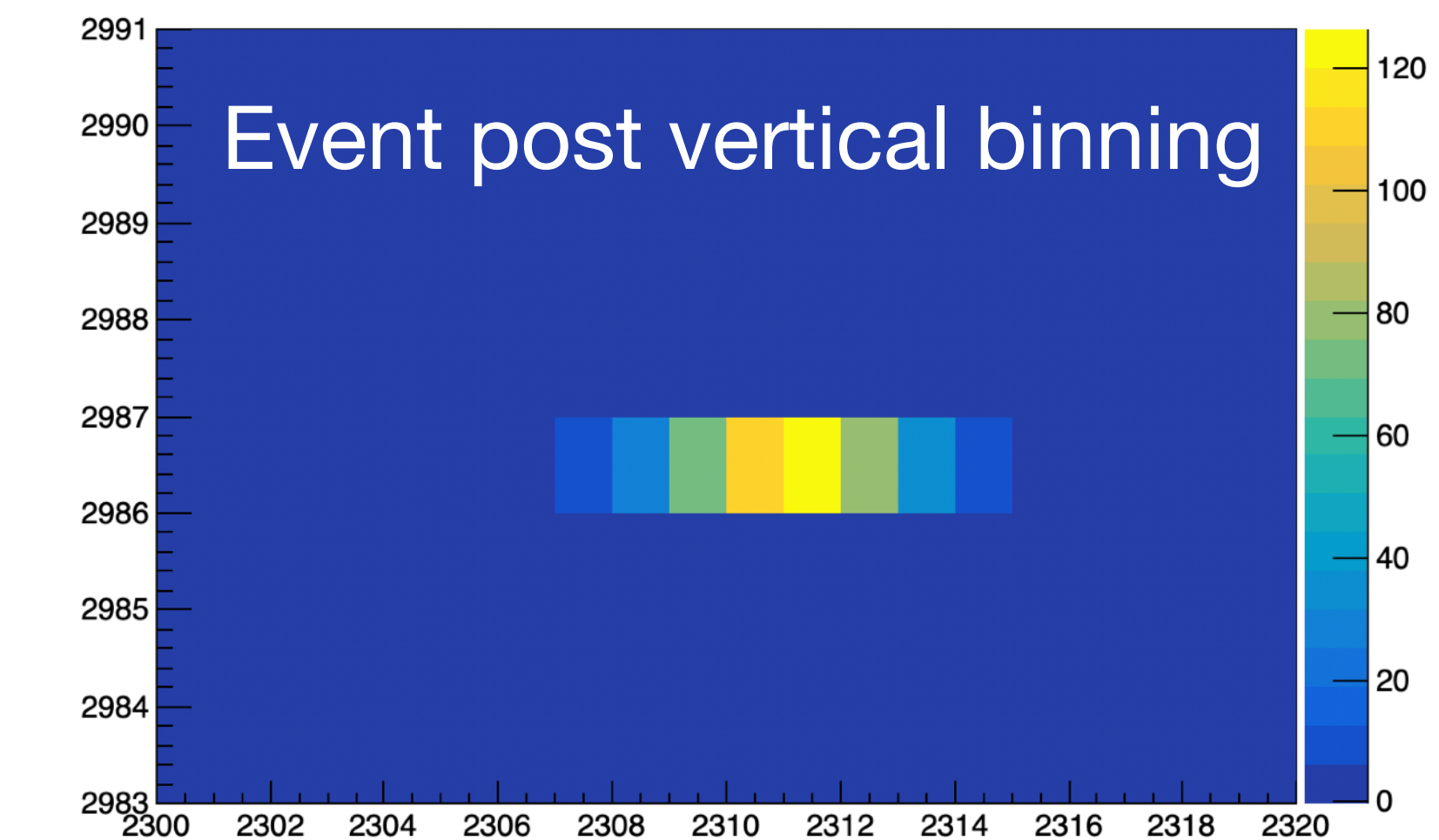
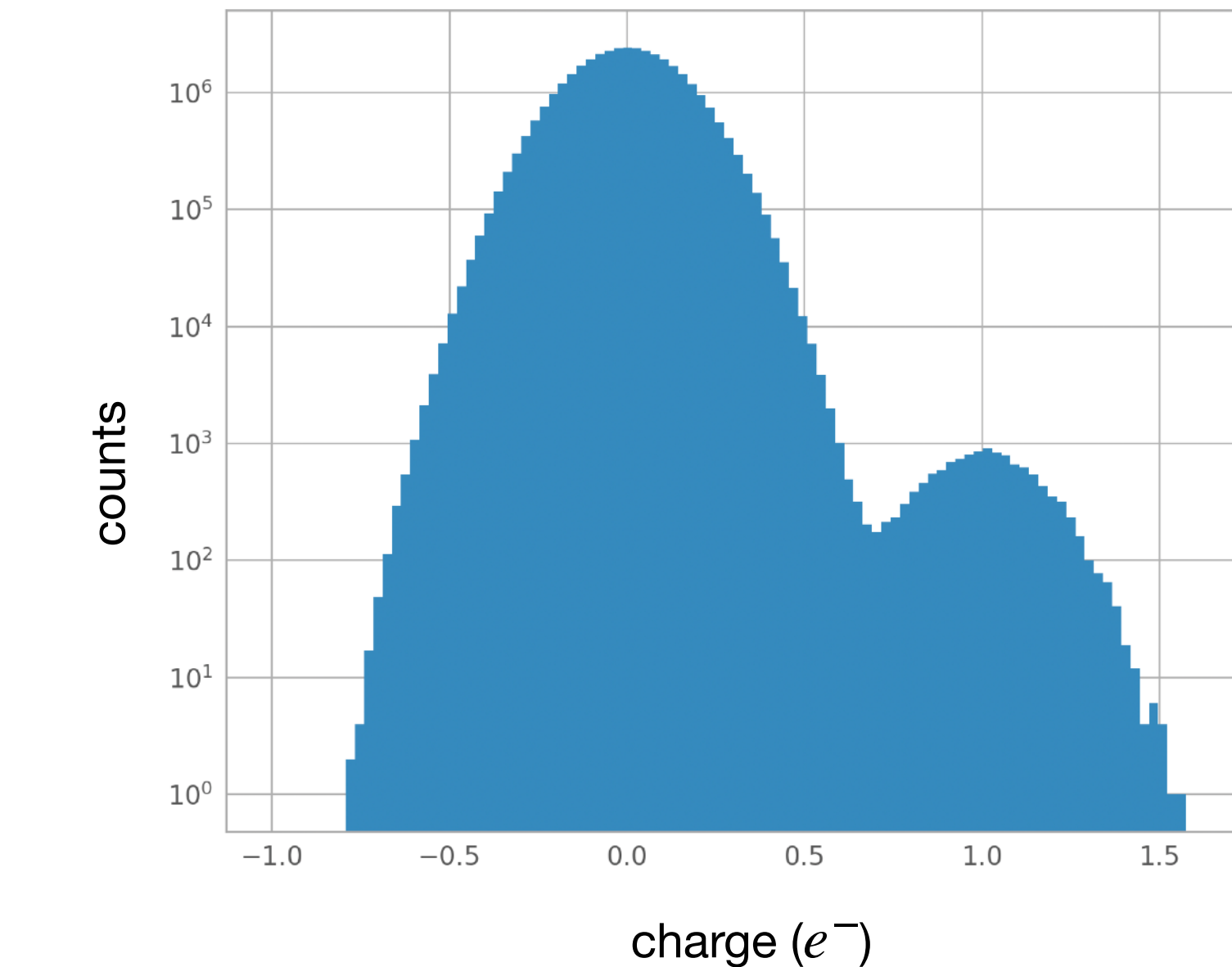


CCD module in Cu box



# Science run 2

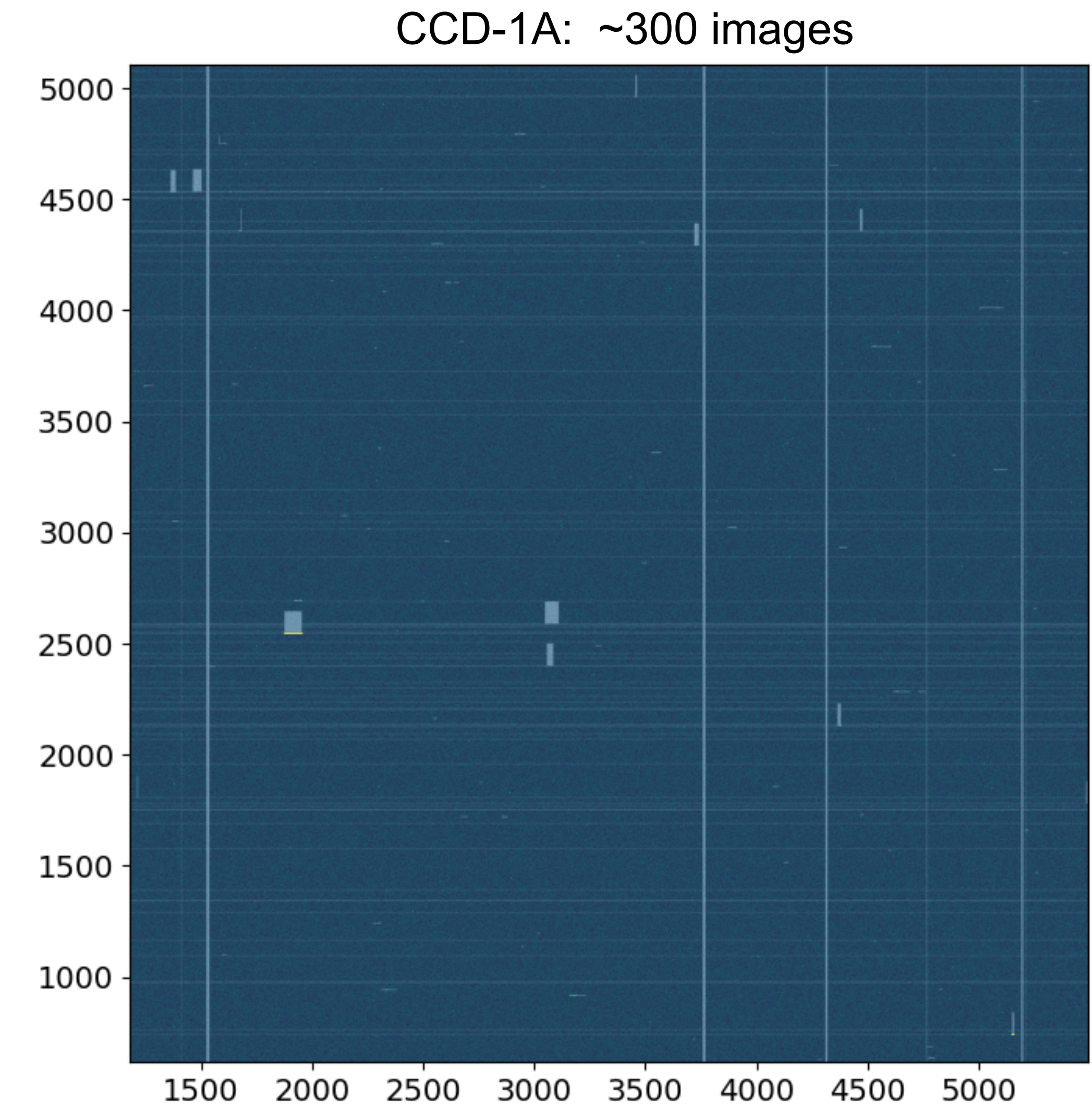
- LBC upgrades post-SR1:
  - 2x CCD modules: 8x 9-Mpixel CCDs, total mass:  $\sim 26$  g.
  - EFCu lids for copper box. Improved light-tightness.
  - DAMIC-M low-noise electronics.
- SR2 readout parameters:
  - Continuous readout. 1 amplifier per CCD.
  - Pixel binning: 1x100.
- Performance:
  - Readout noise:  $0.16e^-$  with 500 NDCM.
  - Reduced dark current:  $5 \times 10^{-3} \rightarrow 10^{-4} e^-/\text{pix/day}$ .



# Data selection criteria

- Dataset 1: to establish selections (139 g-day).
- Selected out:
  - Hot columns.
  - Clusters with total charge  $\geq 6e^-$ .
  - Charge-transfer inefficiency: mask 100 rows above any pixel with  $q > 100e^-$  and its row.
  - Cross-talk: pixels in same-module CCDs from high-energy cluster in one CCD.
  - Correlated-noise: pixels in same-module with correlated charge in multiple CCDs.

$$p_{\text{corr}} = -\log \left[ \prod_L F_{q_{i,j,L}}(0) \right]$$



# Pattern analysis

- Dataset 2: blinded analysis (1.26 kg-day, ~95% sel. efficiency).
- Candidate selection:
  - Horizontal consecutive pixels with total charge 2, 3 and  $4e^-$ .  $p_{mn} = -\log[F_{q_{i,j}}(m)F_{q_{i+1,j}}(n)]$
  - Efficiency: probability of pattern from ionization event with total charge  $N_{e^-}$ . the efficiency for a (2, 3, 4, 5)  $e^-$  as a pattern is  $\sim(38, 65, 79, 86)\%$ ,
- Backgrounds:
  - Random coincidence of uncorrelated-pixel patterns.
  - Radiogenic, scaled from high energies (2.5 to 7.5 keV).

$$B_p^{\text{rad}} = \tau_p N_{\text{obs}}^{\text{rad}}$$

	Pattern $p$		
	{11}	{21}	{111}
$D_p$	144	0	0
$B_p^{\text{rc}}$	141.4	0.111	0.042
$B_p^{\text{rad}}$	0.039	0.039	0.016
	{31}	{22}	{211}
$D_p$	1	0	0
$B_p^{\text{rc}}$	0.019	$2.5 \cdot 10^{-5}$	$5.8 \cdot 10^{-5}$
$B_p^{\text{rad}}$	0.052	0.011	0.035

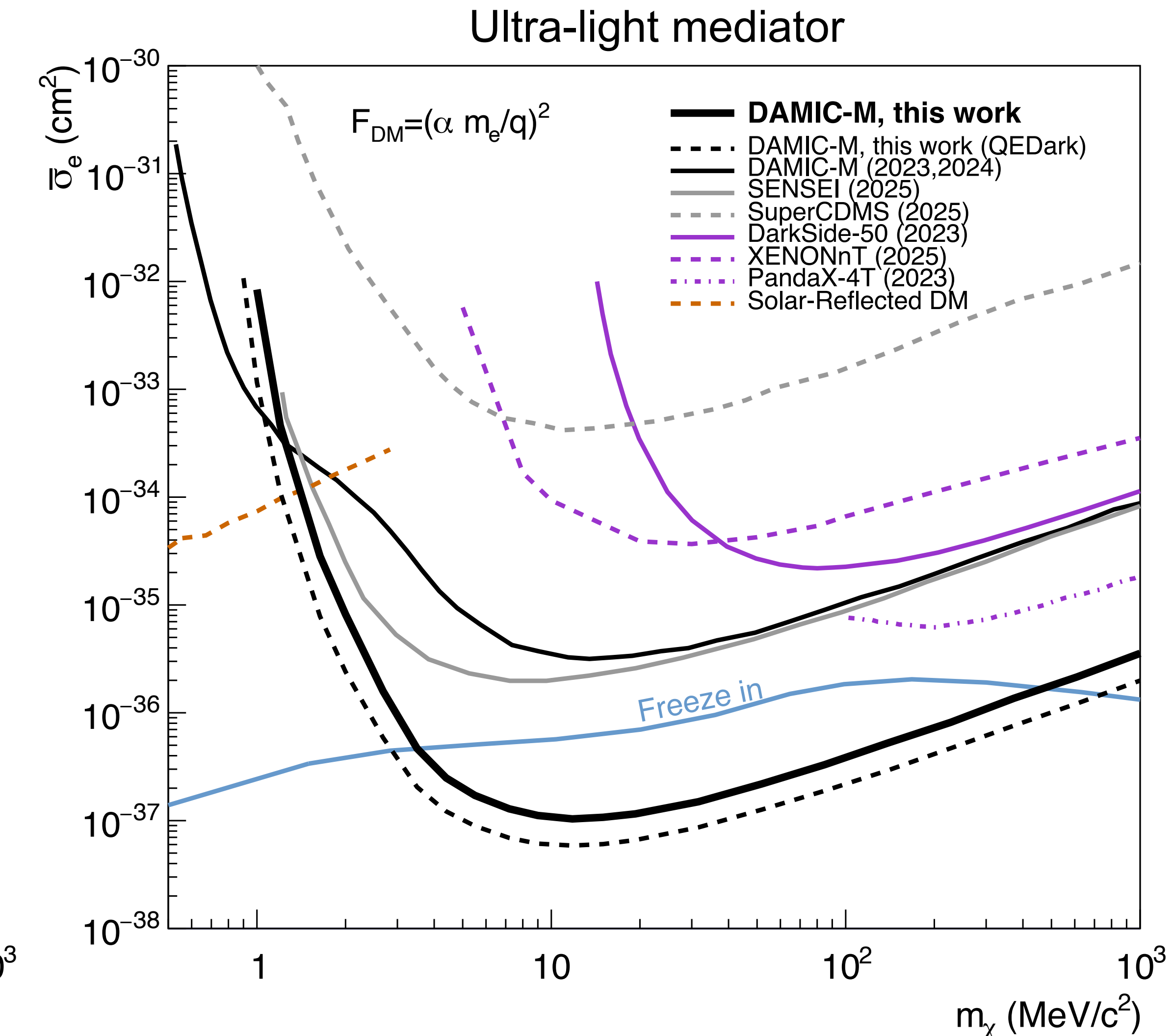
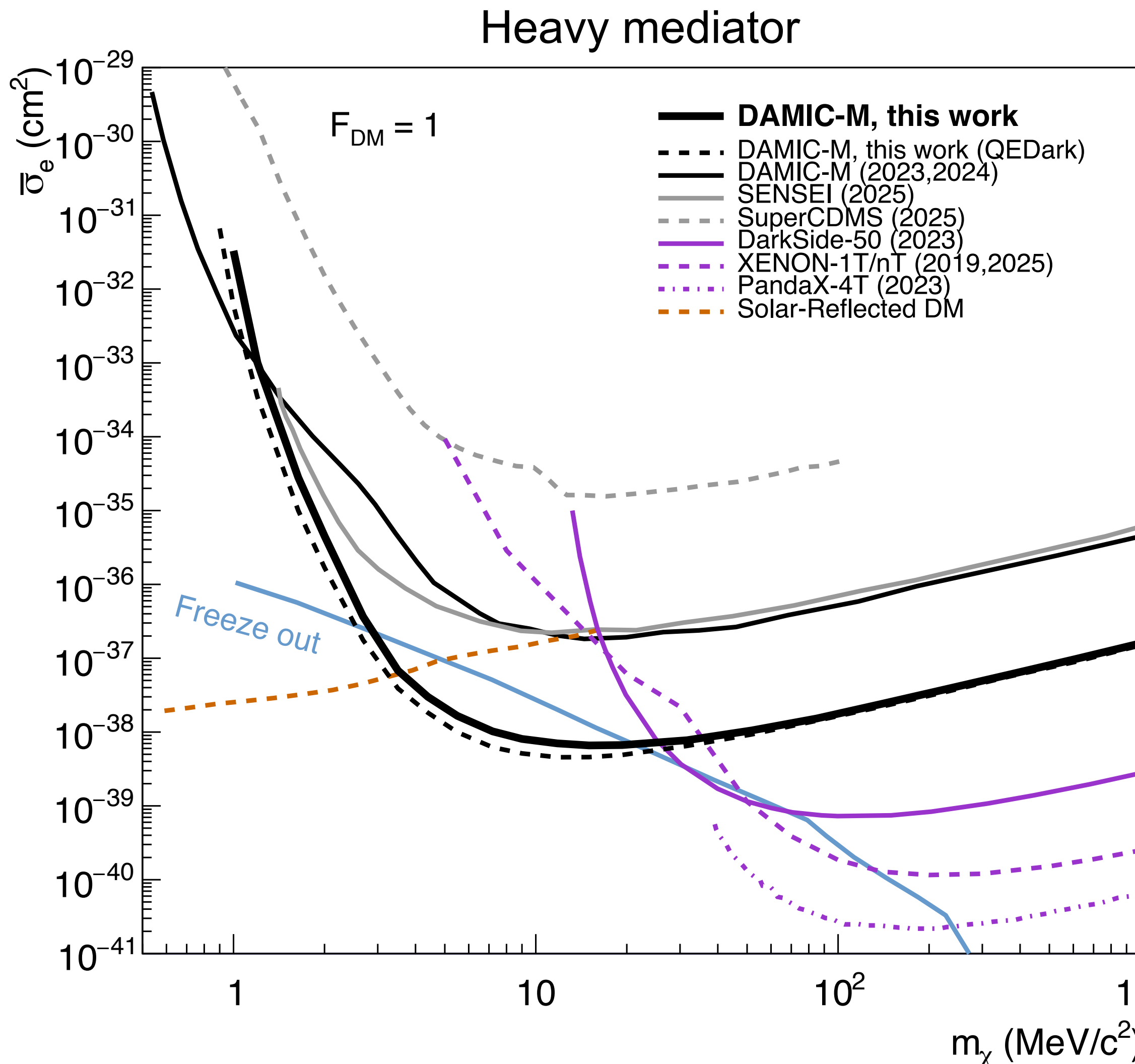
TABLE I. The number of candidates  $D_p$  in the D2 data set, and the number expected from backgrounds due to random coincidences,  $B_p^{\text{rc}}$ , and to radioactive decays,  $B_p^{\text{rad}}$ .

-0.21	0.31	0.03	0.09	0.02	-0.22	-0.06	-0.05	0.22	0.02	-0.15	0.11	0.10	-0.14	-0.05	0.24	0.07	0.11	0.03	-0.06	-0.11	0.16
-0.07	0.04	0.16	-0.07	0.37	-0.06	-0.08	0.04	0.02	0.03	0.08	-0.29	-0.15	0.02	0.21	0.21	-0.09	0.01	0.01	-0.03	0.13	-0.14
0.40	-0.19	-0.01	-0.22	-0.17	-0.01	-0.07	0.10	-0.08	0.03	-0.09	0.01	-0.15	-0.02	0.26	0.13	0.09	0.23	0.18	-0.17	0.33	
0.06	-0.13	0.26	-0.18	-0.01	0.12	0.13	0.14	0.15	-0.27	0.10	0.42	-0.10	0.10	0.11	0.08	0.26	0.21	0.29	0.14	0.06	0.35
-0.06	0.22	0.01	0.04	1.20	1.15	0.16	-0.11	0.01	0.06	-0.17	-0.13	-0.17	0.26	0.14	0.33	-0.21	0.11	0.02	-0.15	0.07	-0.14
0.24	-0.08	0.05	0.01	0.37	-0.23	0.20	0.00	-0.00	-0.01	0.24	0.06	-0.13	0.12	0.29	2.99	1.36	0.12	-0.04	0.03	0.07	0.18
-0.05	0.10	0.07	-0.03	0.05	-0.20	-0.12	-0.22	-0.05	-0.11	0.08	-0.12	0.09	-0.10	0.10	0.24	0.21	0.13	0.09	0.08	0.07	0.15
0.05	-0.13	-0.12	-0.13	0.12	-0.15	0.13	-0.18	0.07	-0.02	-0.22	0.05	0.17	-0.23	-0.18	0.17	-0.36	-0.37	-0.33	-0.31	-0.19	
0.03	-0.10	0.16	0.15	-0.20	0.07	0.20	0.08	-0.19	-0.11	0.08	-0.13	-0.02	0.02	-0.29	-0.05	-0.16	0.10	0.09	0.27	0.08	0.08
0.09	-0.02	0.19	0.04	0.16	-0.28	-0.04	-0.18	0.13	-0.00	0.14	0.19	0.08	-0.12	0.20	0.21	-0.03	0.42	-0.10	-0.16	0.30	-0.03

{1,1} and {3,1} candidates.

# DAMIC-M exclusion limits

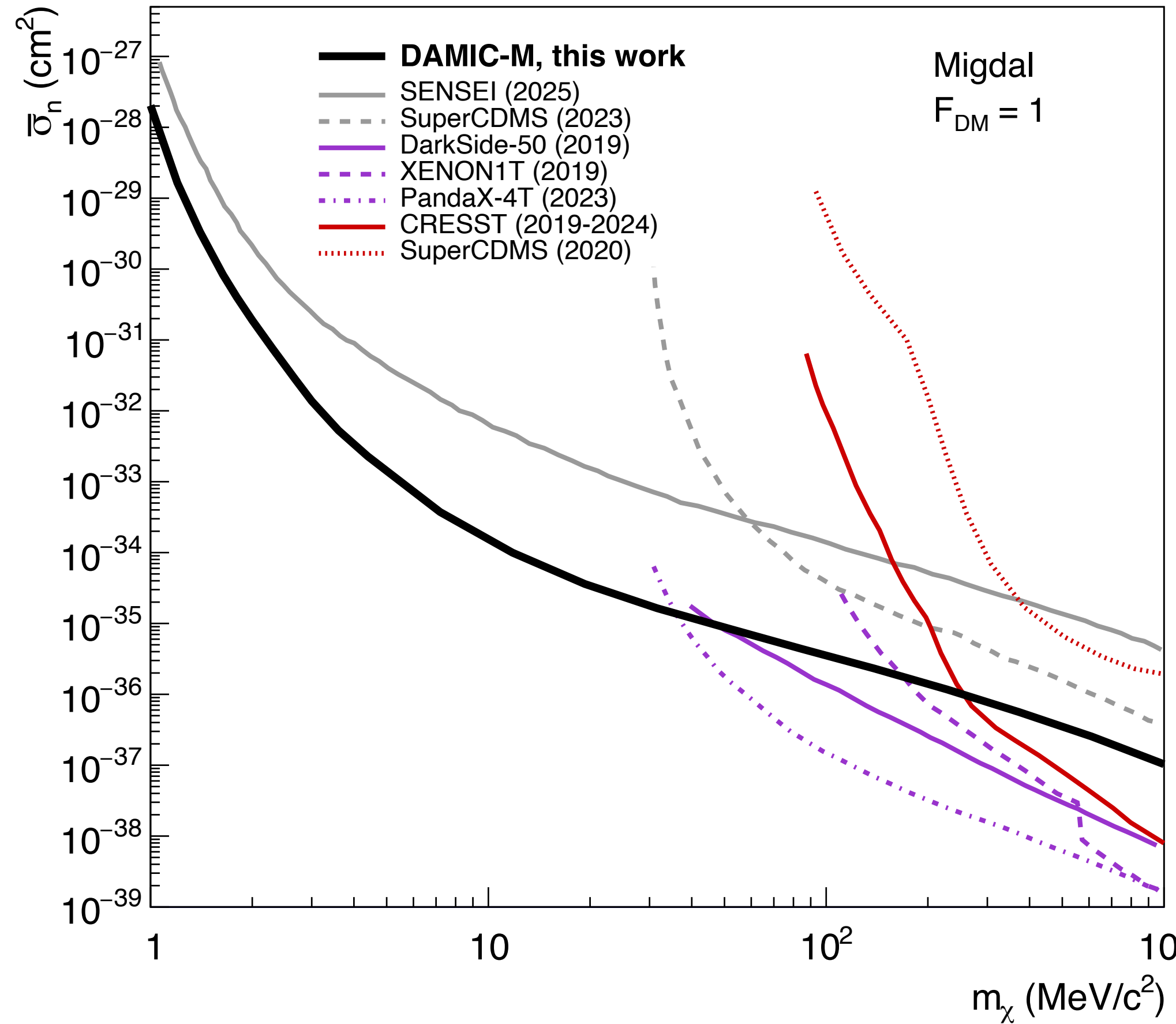
PRL135(2025)071002



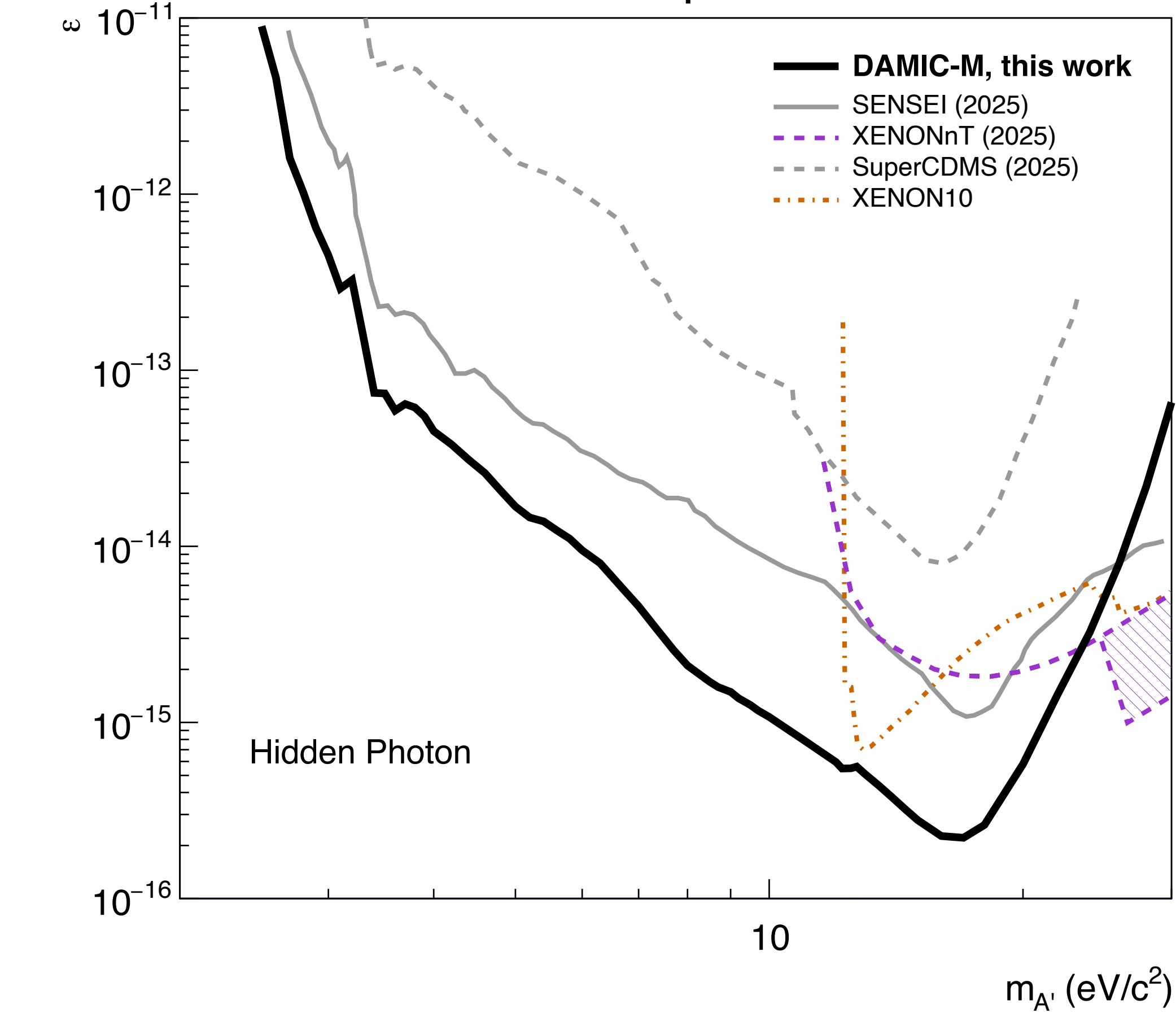
# DAMIC-M exclusion limits

PRL135(2025)071002

Migdal via DM-nucleus scattering



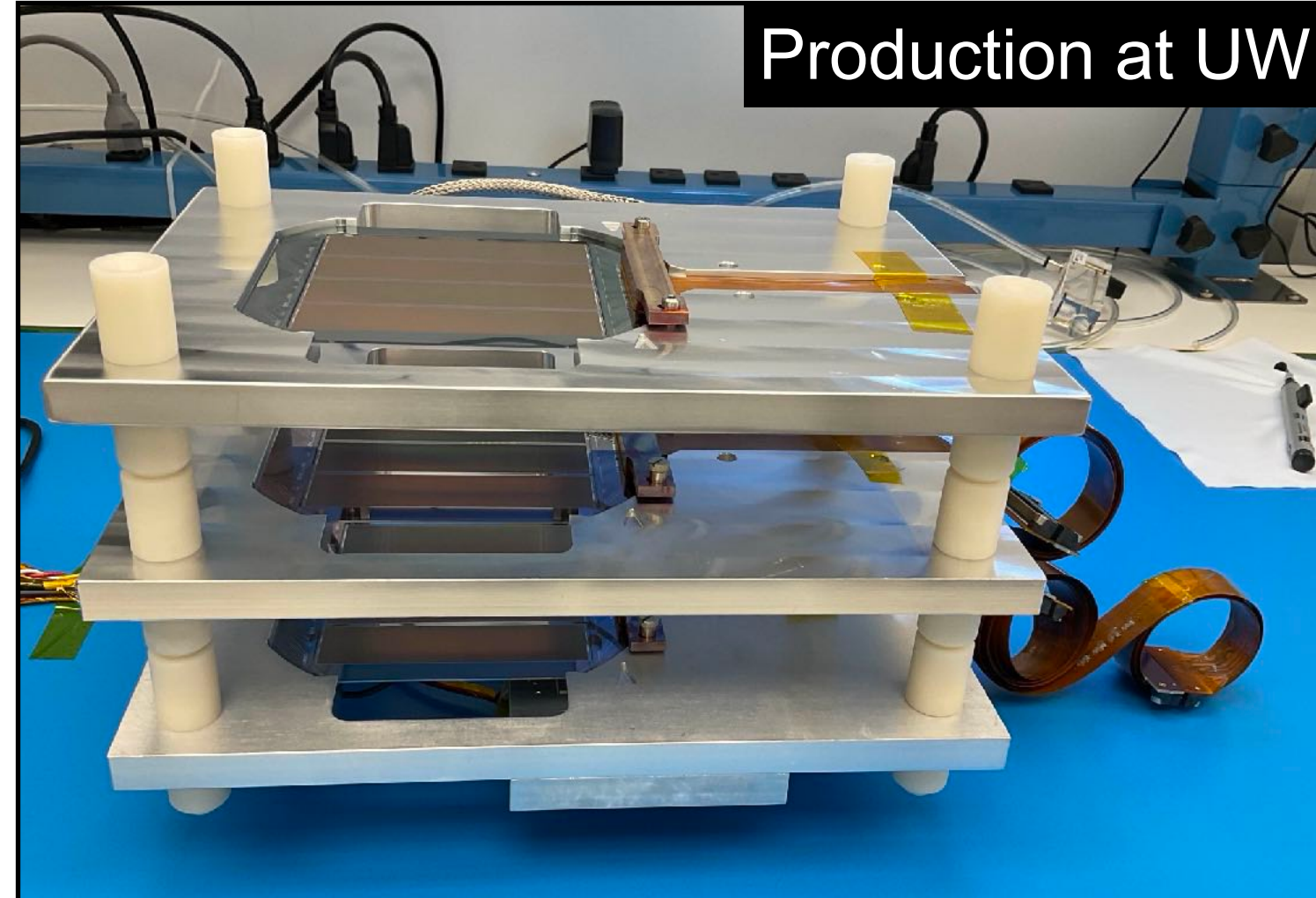
Hidden photon



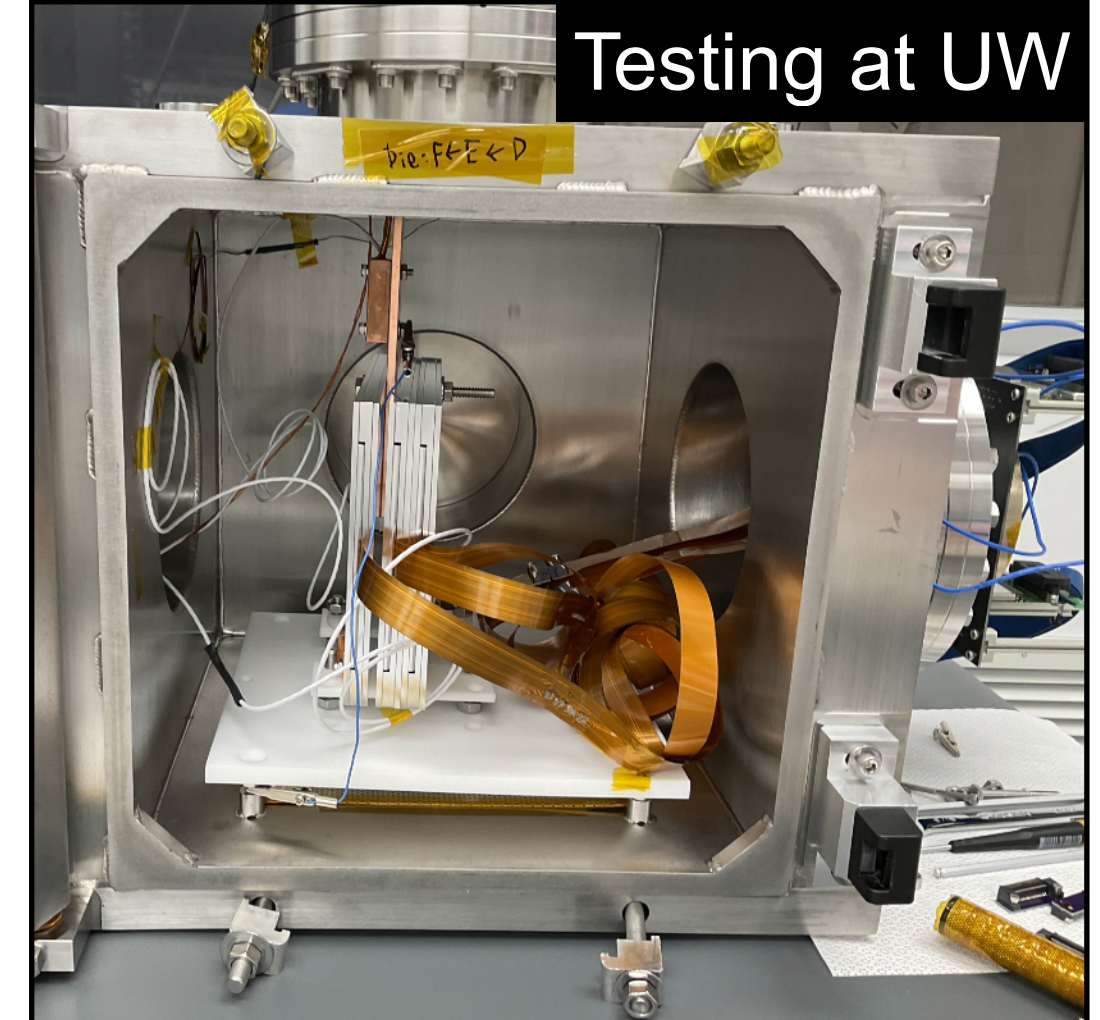
# DAMIC-M status

Soon on the arXiv!

- CCD module production at UW completed (late 2024).
- Underground characterization before array assembly (ongoing).
- Copper machining ongoing, lead and poly shield ready.
- Production electronics testing ongoing.
- Detector installation in early 2026!



Production at UW



Testing at UW



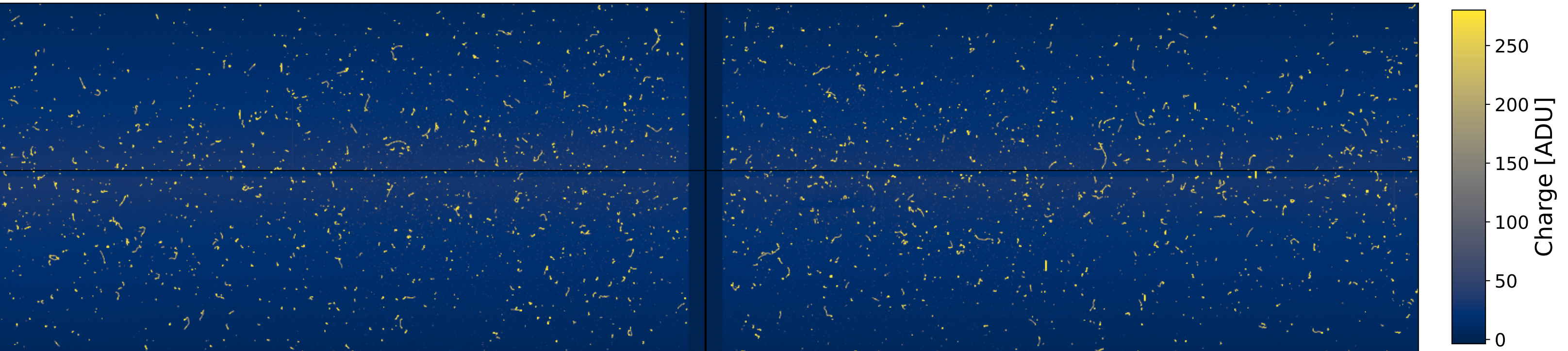
Shielded container @ reception



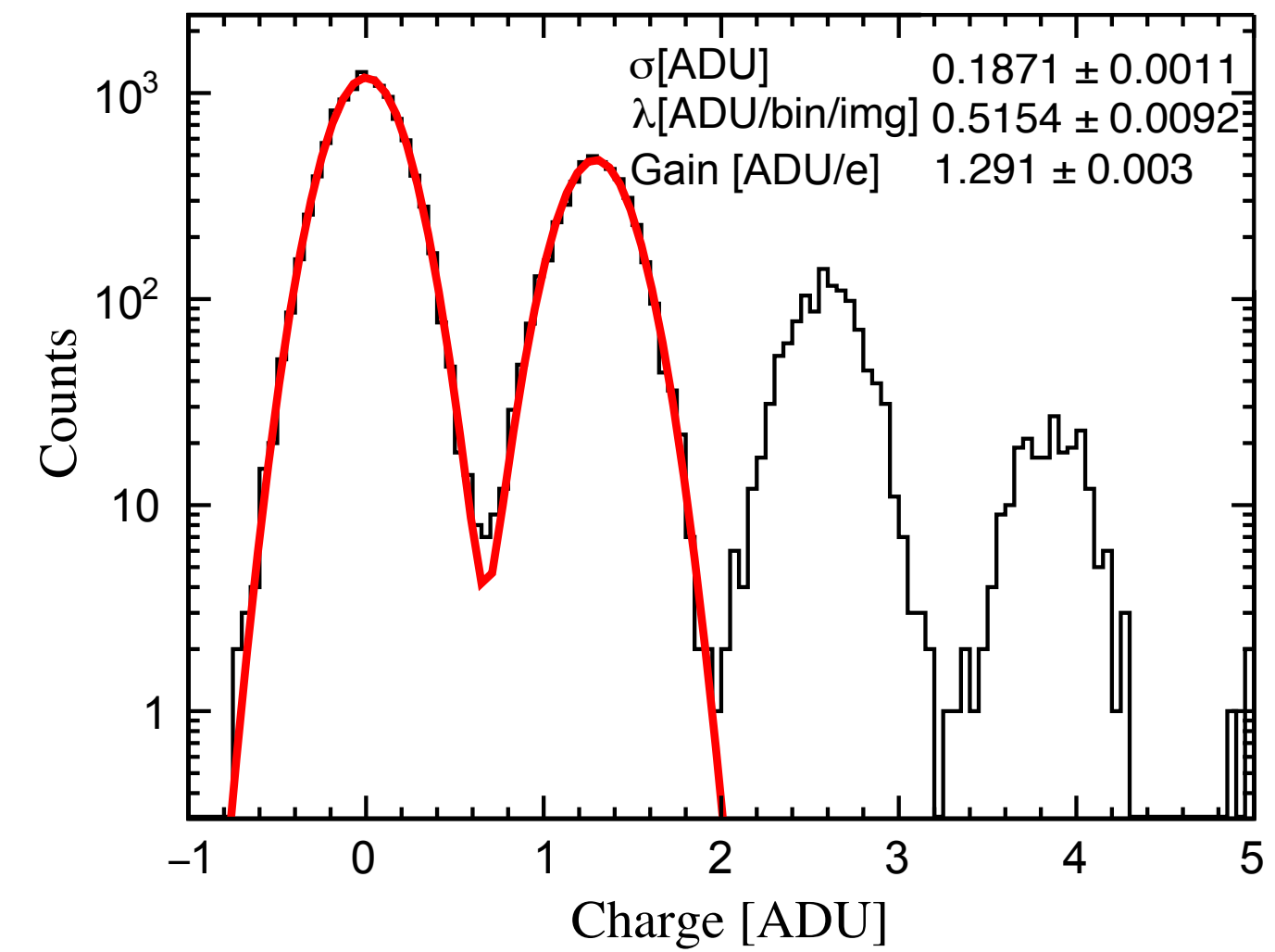
Testing at LSM (ongoing)

# Snapshots from testing at LSM

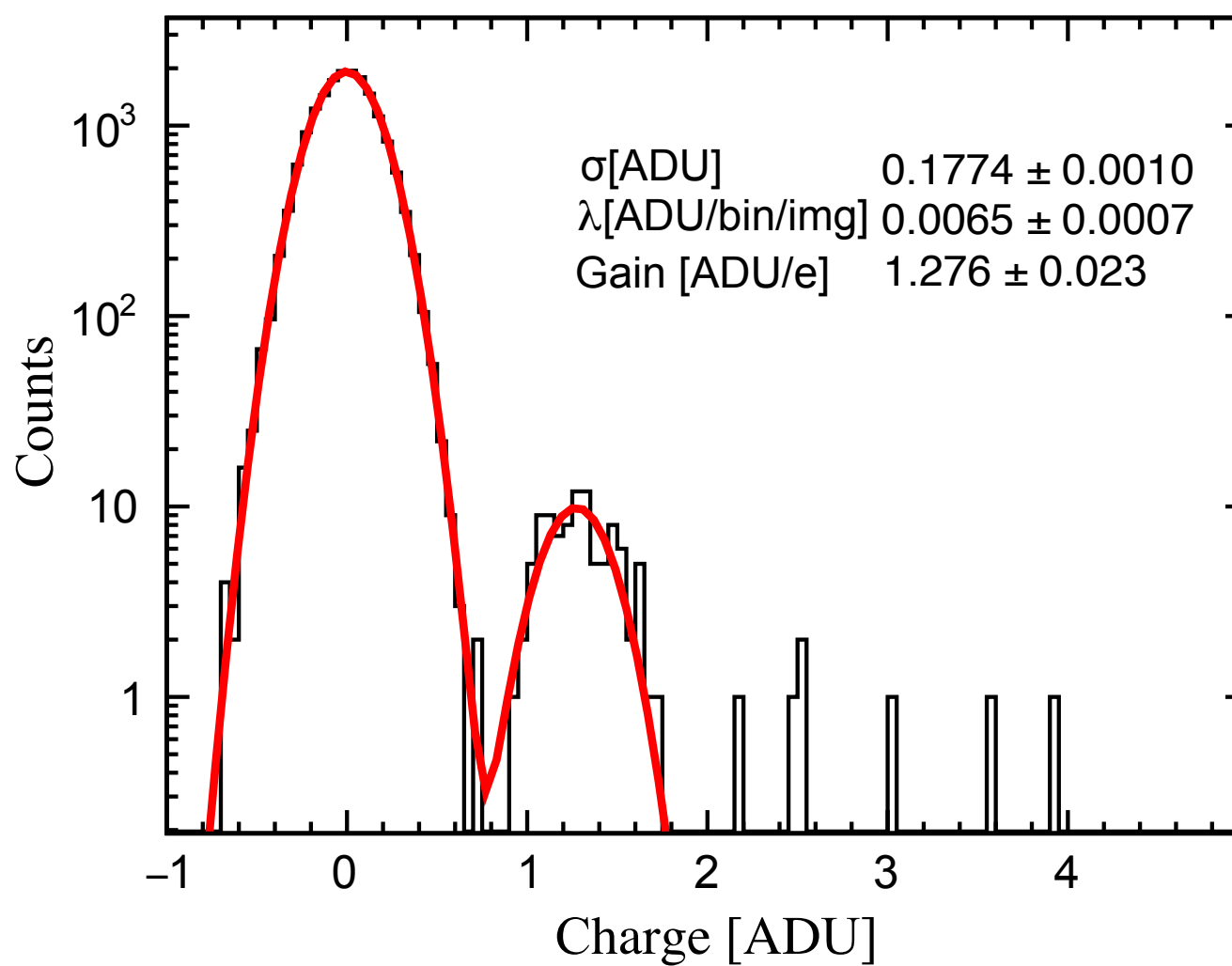
- In-depth characterization of DAMIC-M “DM” modules.
- Testing protocols optimized for underground.



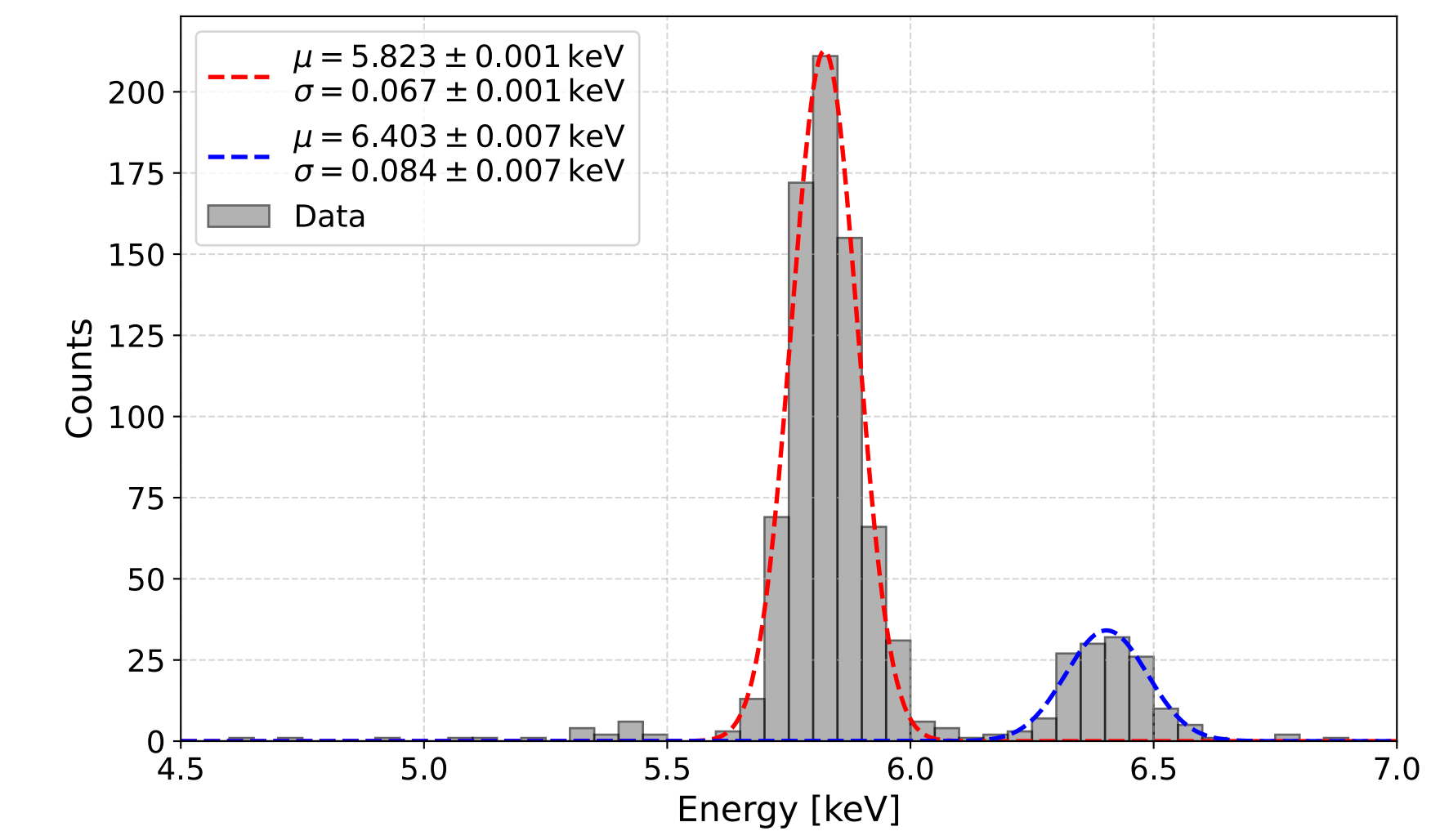
DM-03 image (4 CCDs).



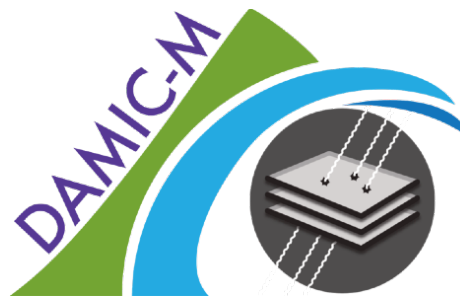
PCD at 185 K



PCD at 135 K

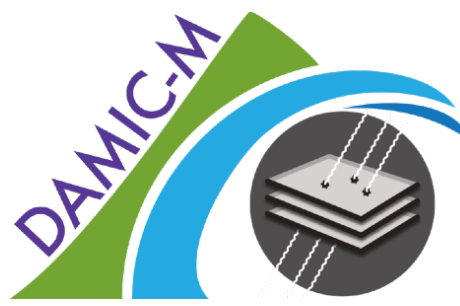


Fe-55 calibration



# Conclusions

- With this search, DAMIC-M establishes the most stringent limits to date on DM particles interacting with electrons between 1 and 1000 MeV. [PRL135\(2025\)071002](#)
- First experiment to rule out that relic DM features ultralight-mediator DM (freeze-in) as a dominant component between 3.5 and 490 MeV.
- Also rules out heavy-mediator scalar DM (freeze-out) in any fraction between 2.9 and 21.5 MeV.
- We fabricated and tested 28 low-background CCD modules at the University of Washington. In depth characterization ongoing at LSM.
- DAMIC-M will be deployed in early 2026.



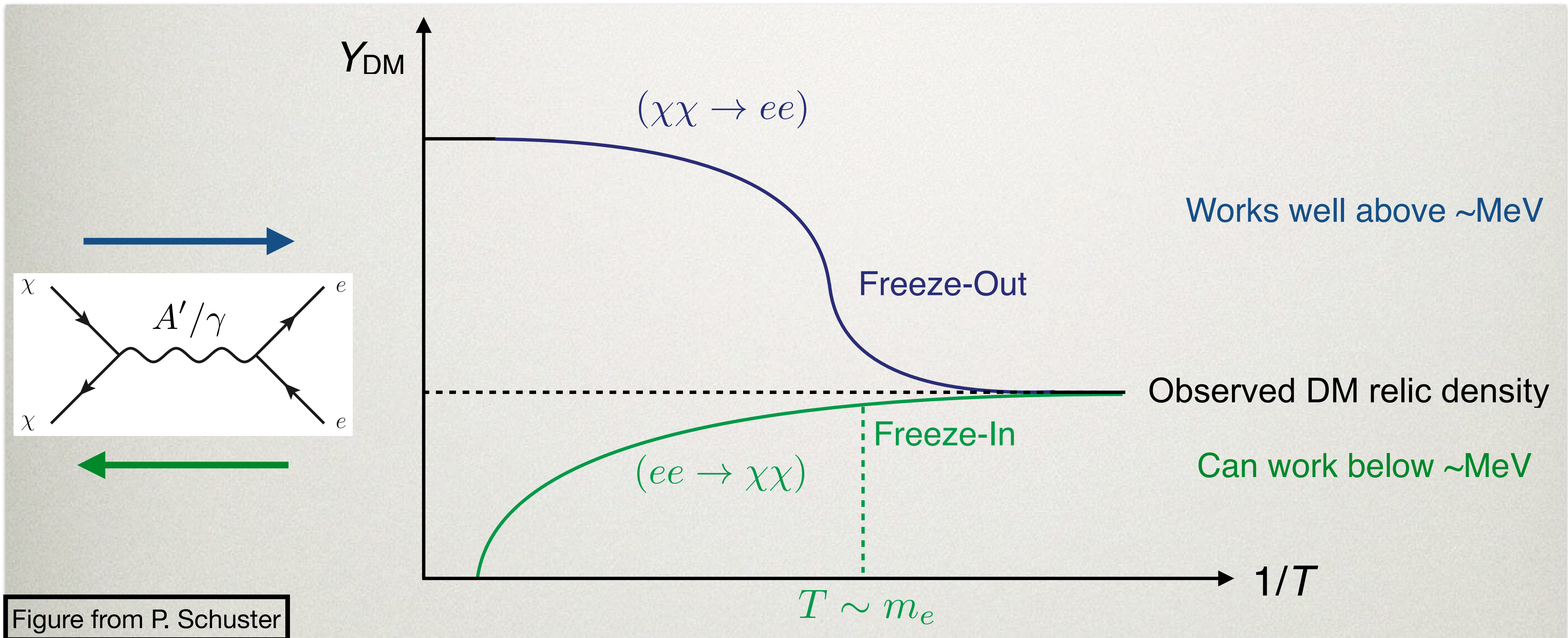


# The DAMIC-M Collaboration



# Relic abundance from the hidden sector

- Hidden-sector DM models can give rise to the observed relic density.



# Signal model and limit

PRD102(2020)063026

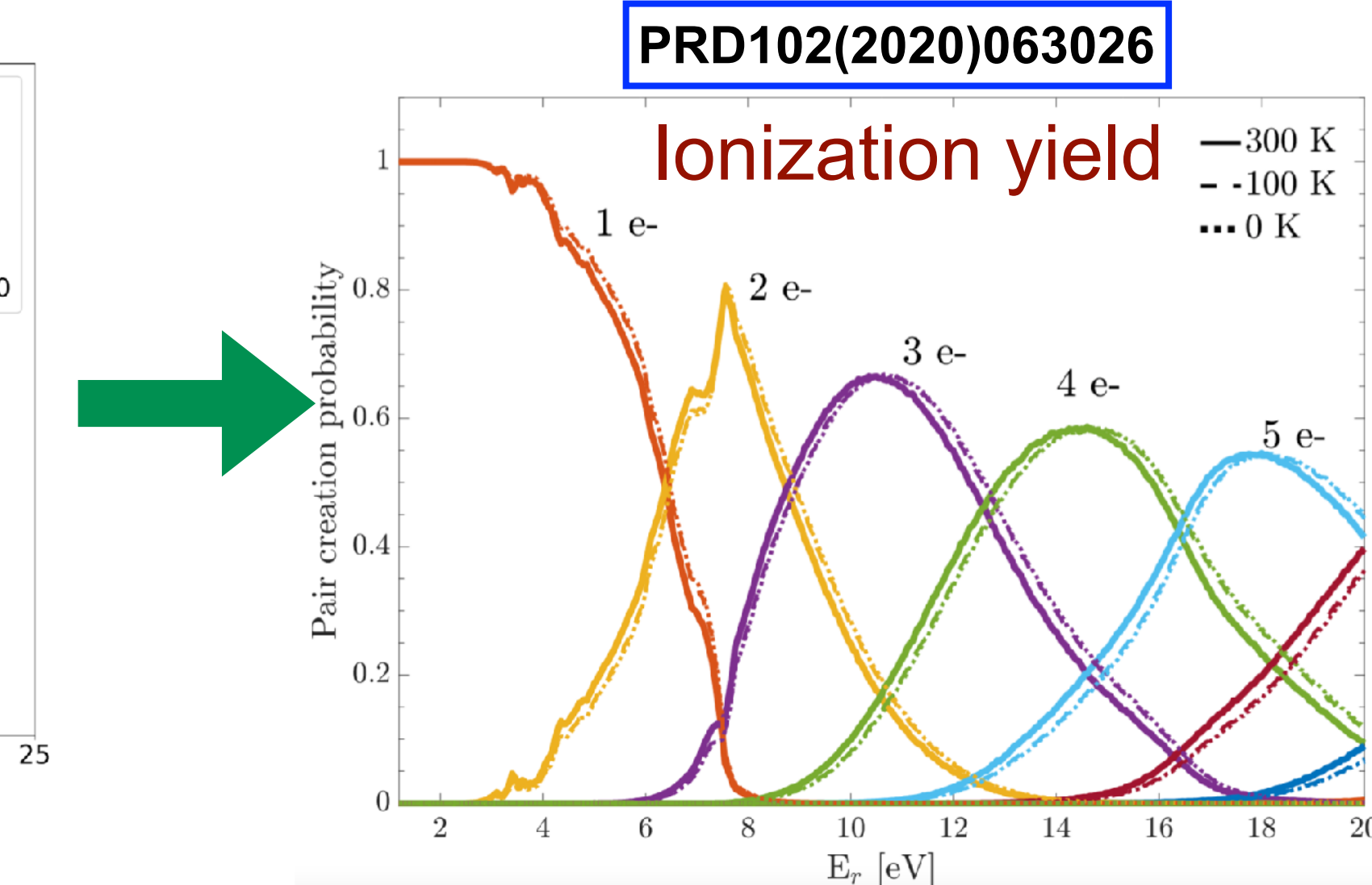
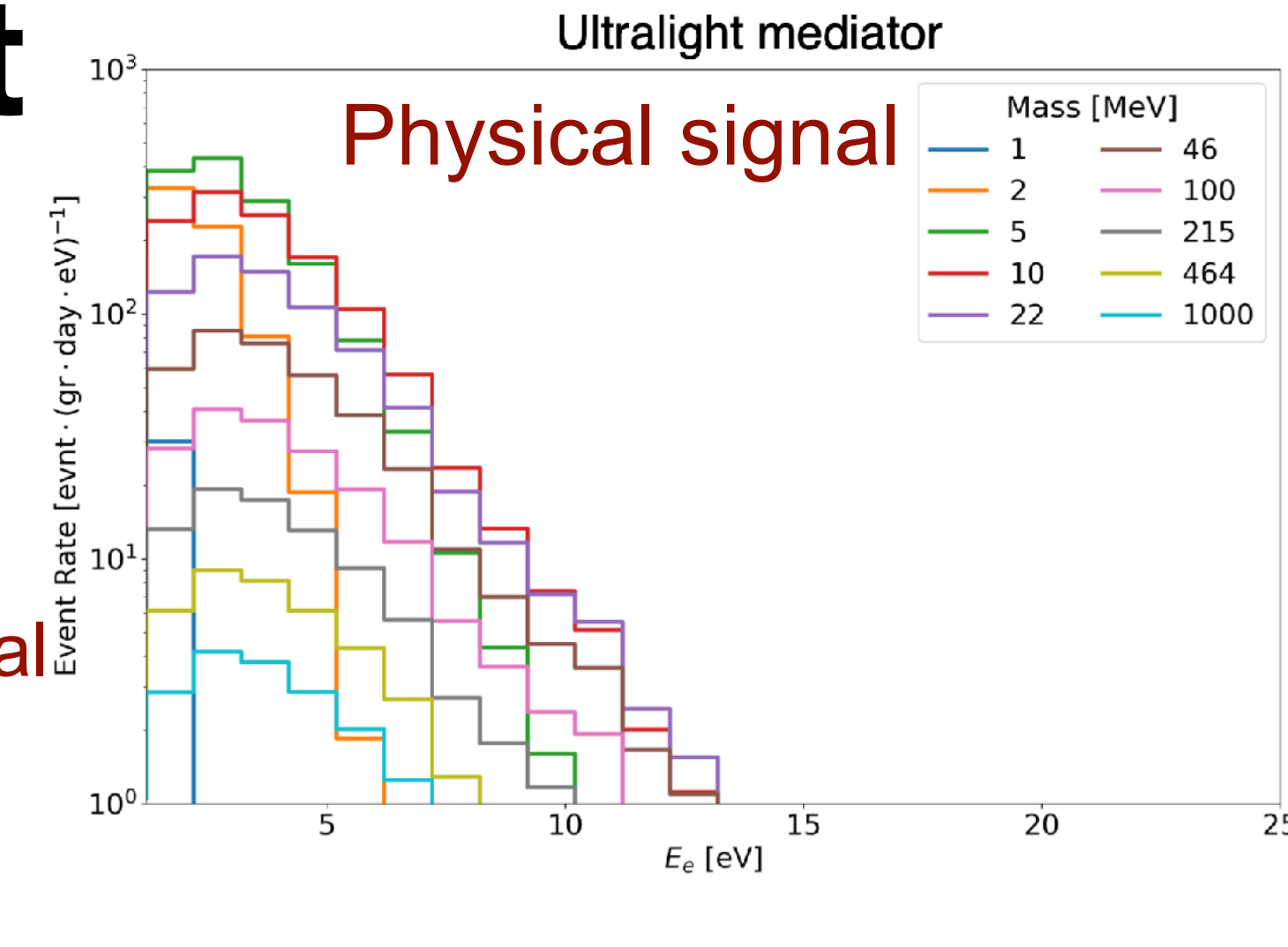
**theory input**

DM-e cross section

$$\frac{dR}{dE_e} \propto \bar{\sigma}_e \int \frac{dq}{q^2} \left[ \int \frac{f(\mathbf{v})}{\mathbf{v}} d^3v \right] |F_{\text{DM}}(q)|^2 |F_c(q, E_e)|^2$$

DM galactic halo

DM form factor crystal



N. of patterns  $p$

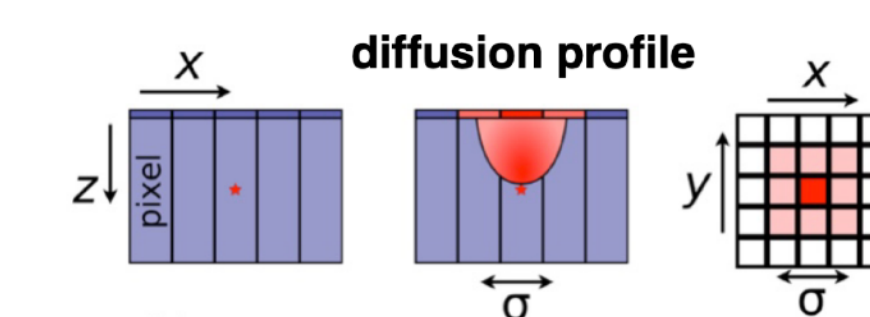
$$S_p = \sum_{q_e} N_{q_e}(\bar{\sigma}_e, m_\chi) P_{q_e \rightarrow p}$$

Probability that  $q_e$  charges result in a pattern  $p$

$\bar{\sigma}_e$  nuisance

$$\mathcal{L}(\mu, \theta) = \prod_p \frac{(S_p(\mu) + B_p^{rc} + \theta B_p^{rad})^{D_p} e^{-(S_p(\mu) + B_p^{rc} + \theta B_p^{rad})}}{D_p!} \prod_p \frac{(\theta \tau_p B_p^{rad})^{N_{rad}} e^{-(\theta \tau_p B_p^{rad})}}{N_{rad}!}$$

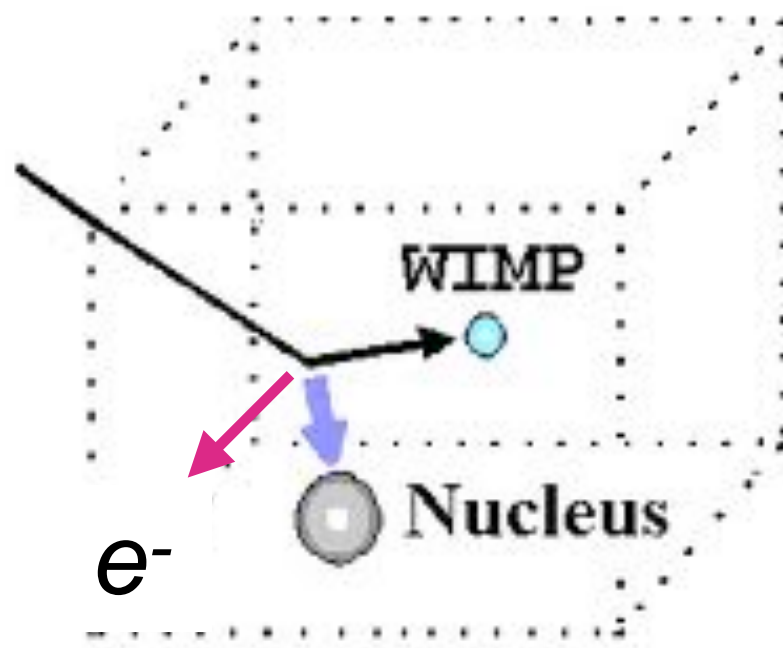
control sample



The background-only null hypothesis has  $p_0 = 0.24$  (0.10), so we place 90% CL exclusion limits using the profile likelihood ratio test statistics.

# Migdal electrons

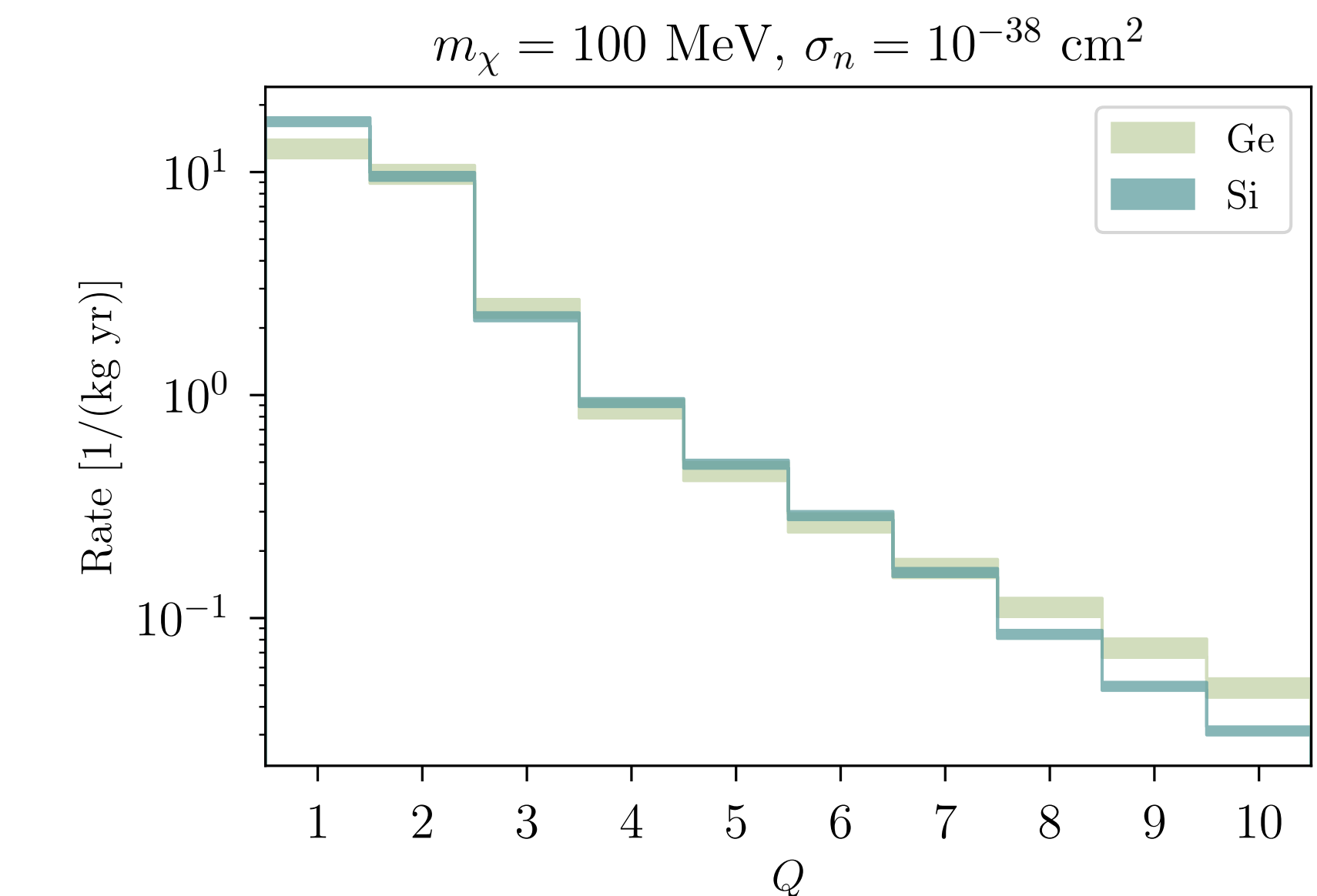
## Three-body final state:



- Migdal effect: an additional (atomic  $e^-$ ) in the final state.
- $E$  and  $p$  conserved even when  $e^-$  takes most of the WIMP kinetic energy.
- Very rare process.
- Not yet observed for keV energies.  
Uncalibrated. We have plans to do it.

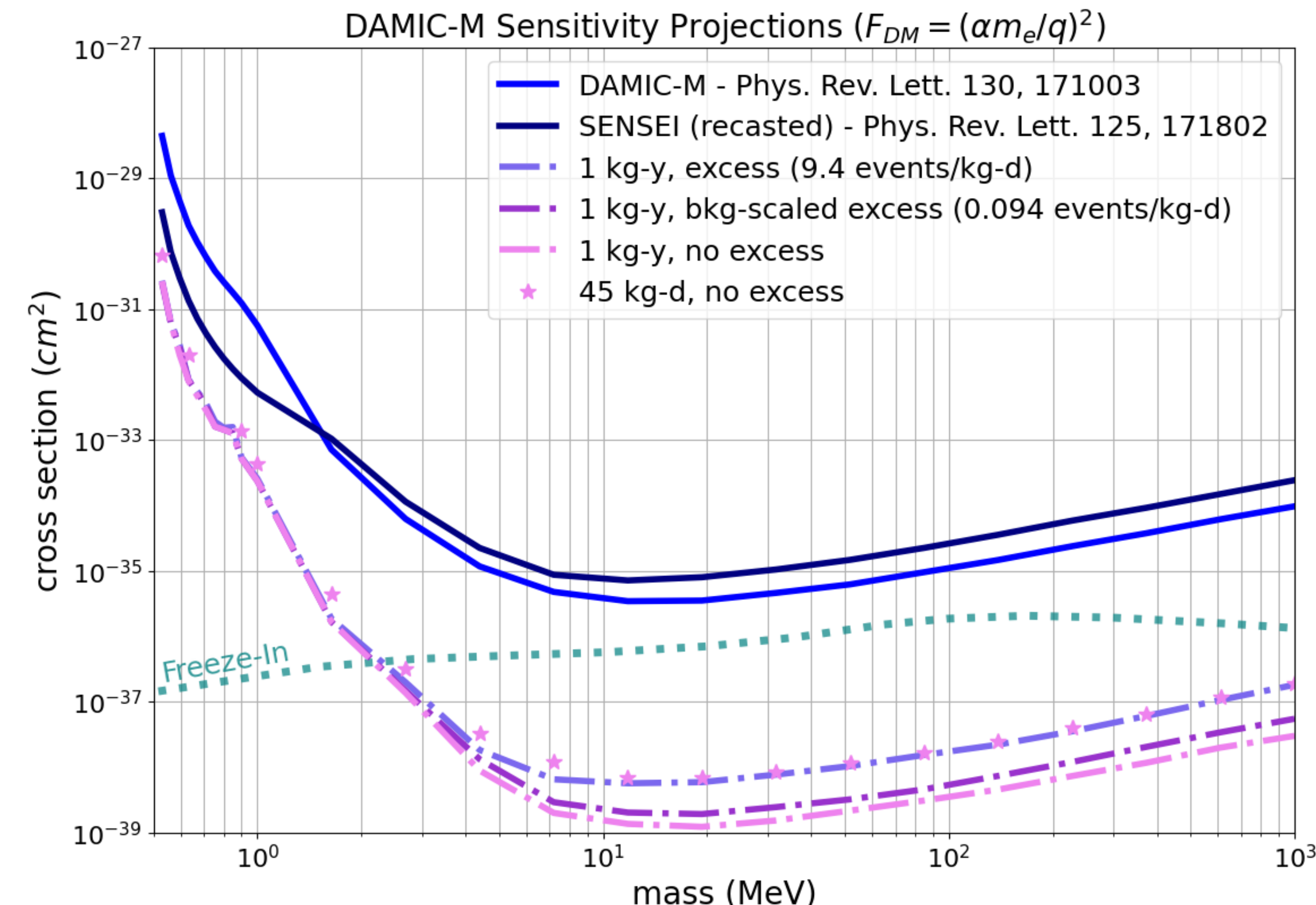
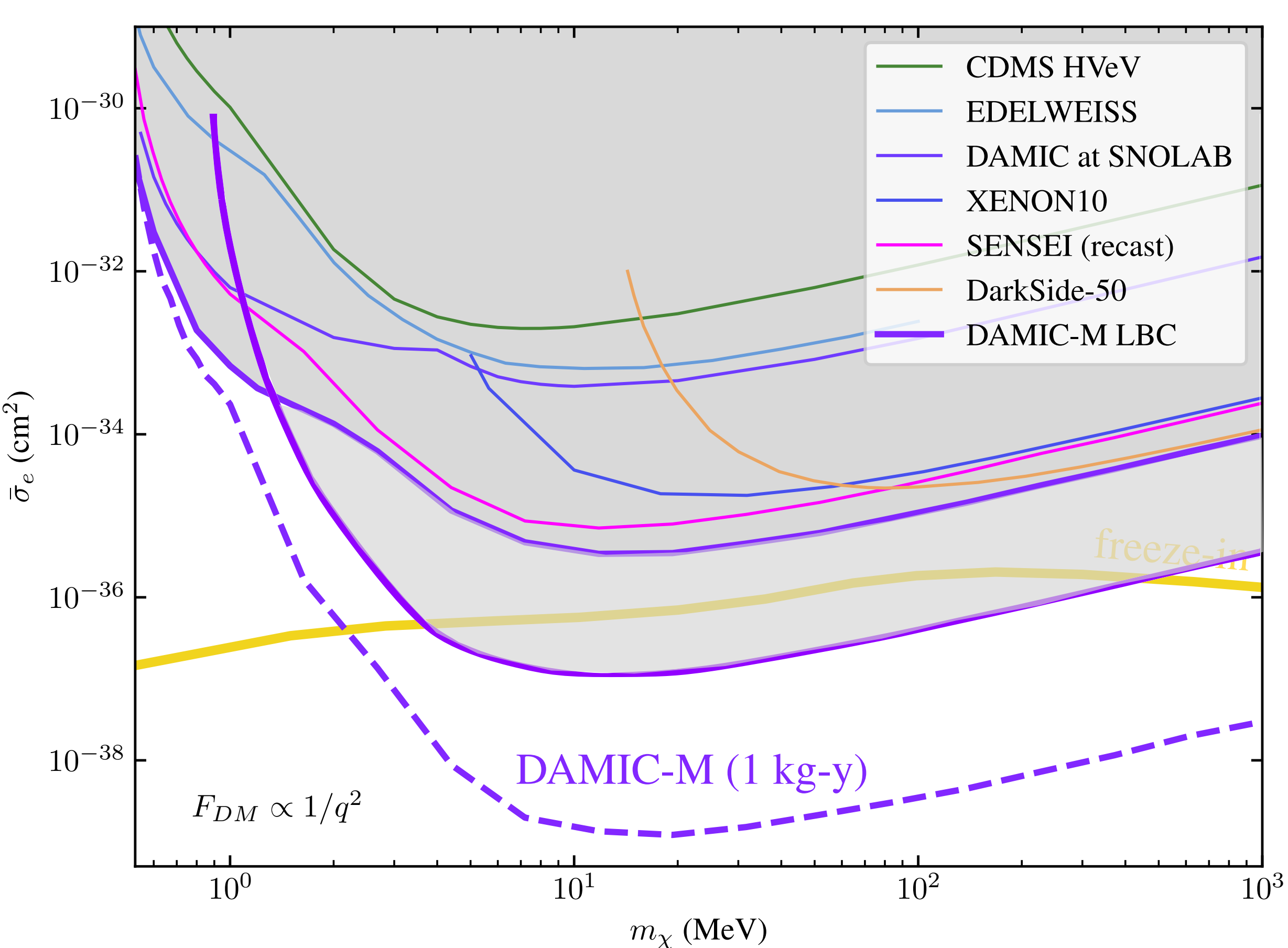
## Bosonic DM absorption:

- DM particle is a boson that couples to the electron, e.g., a “dark” or “hidden” photon.
- DM is absorbed by the target electron and its rest energy released as electronic recoil K.E.



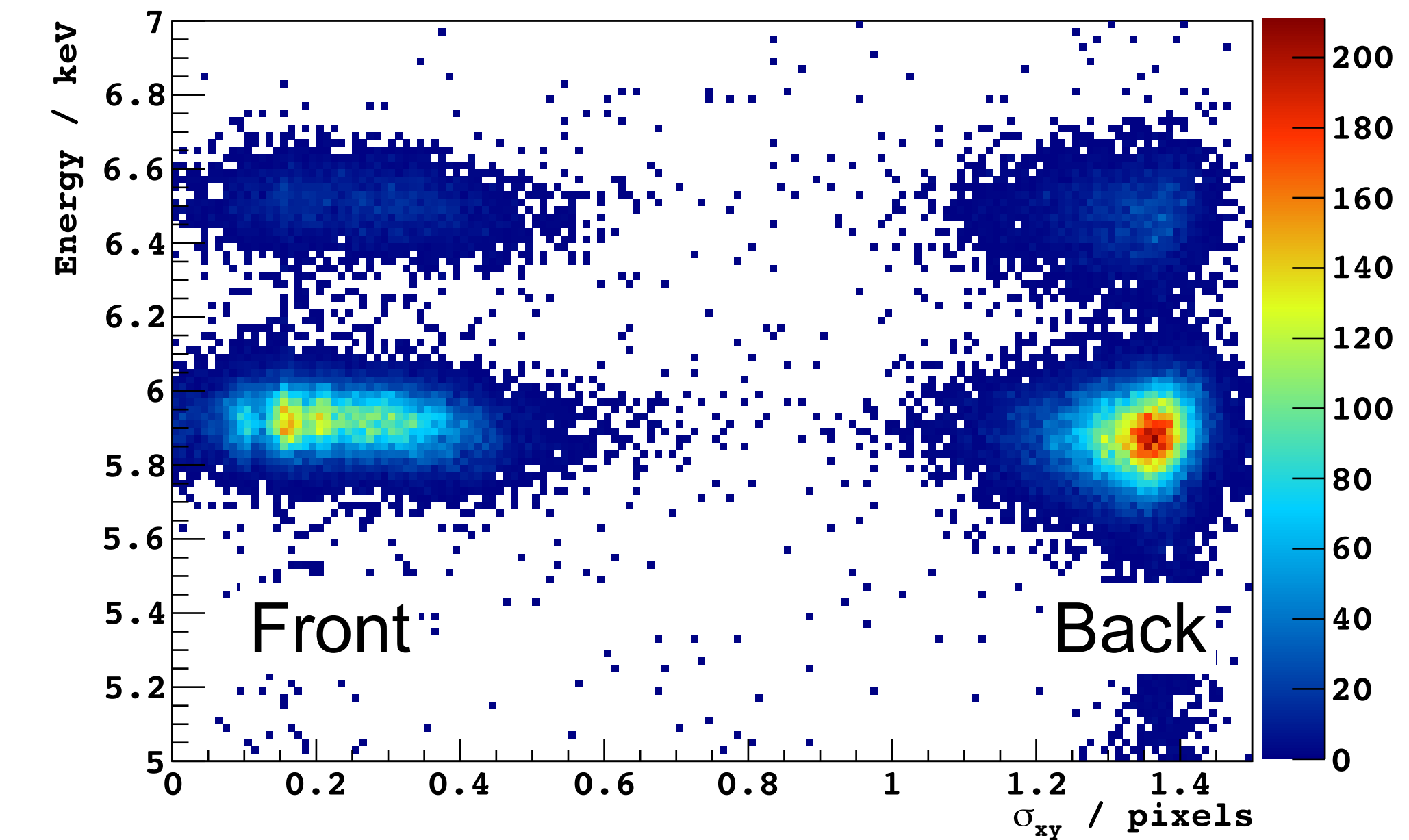
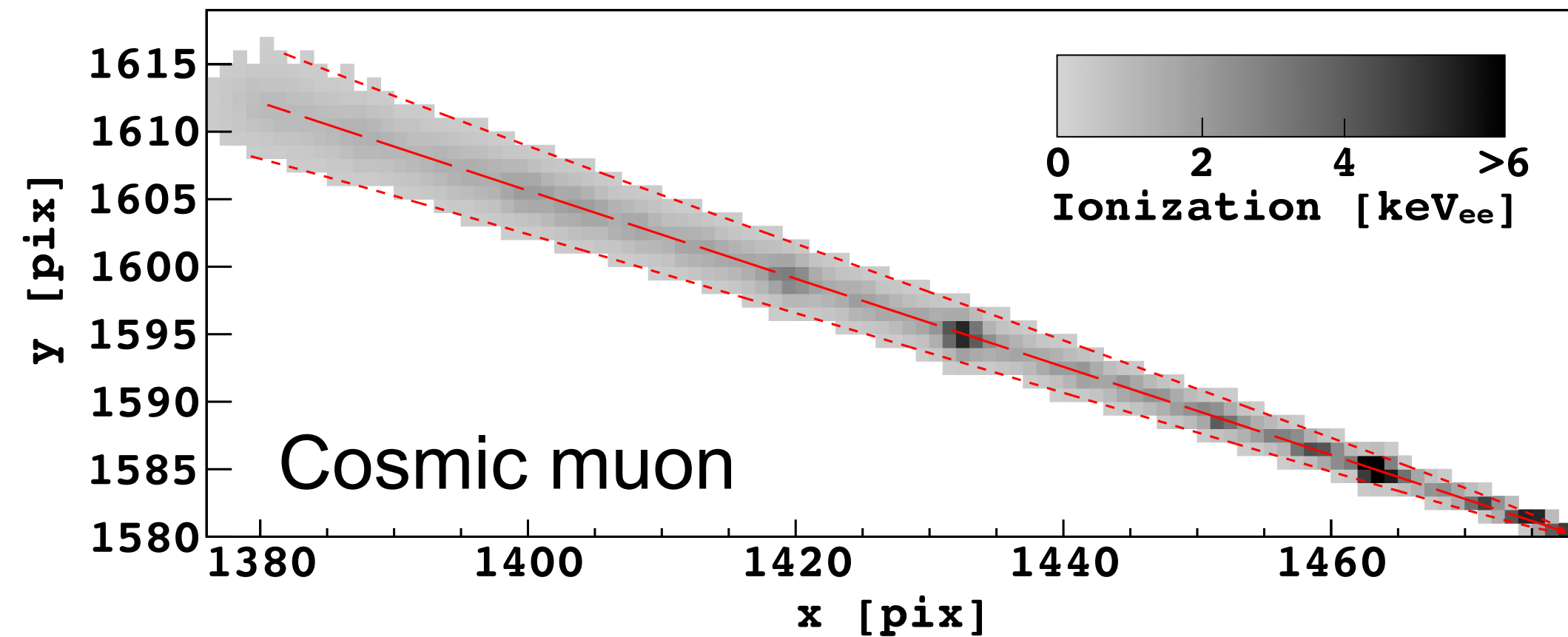
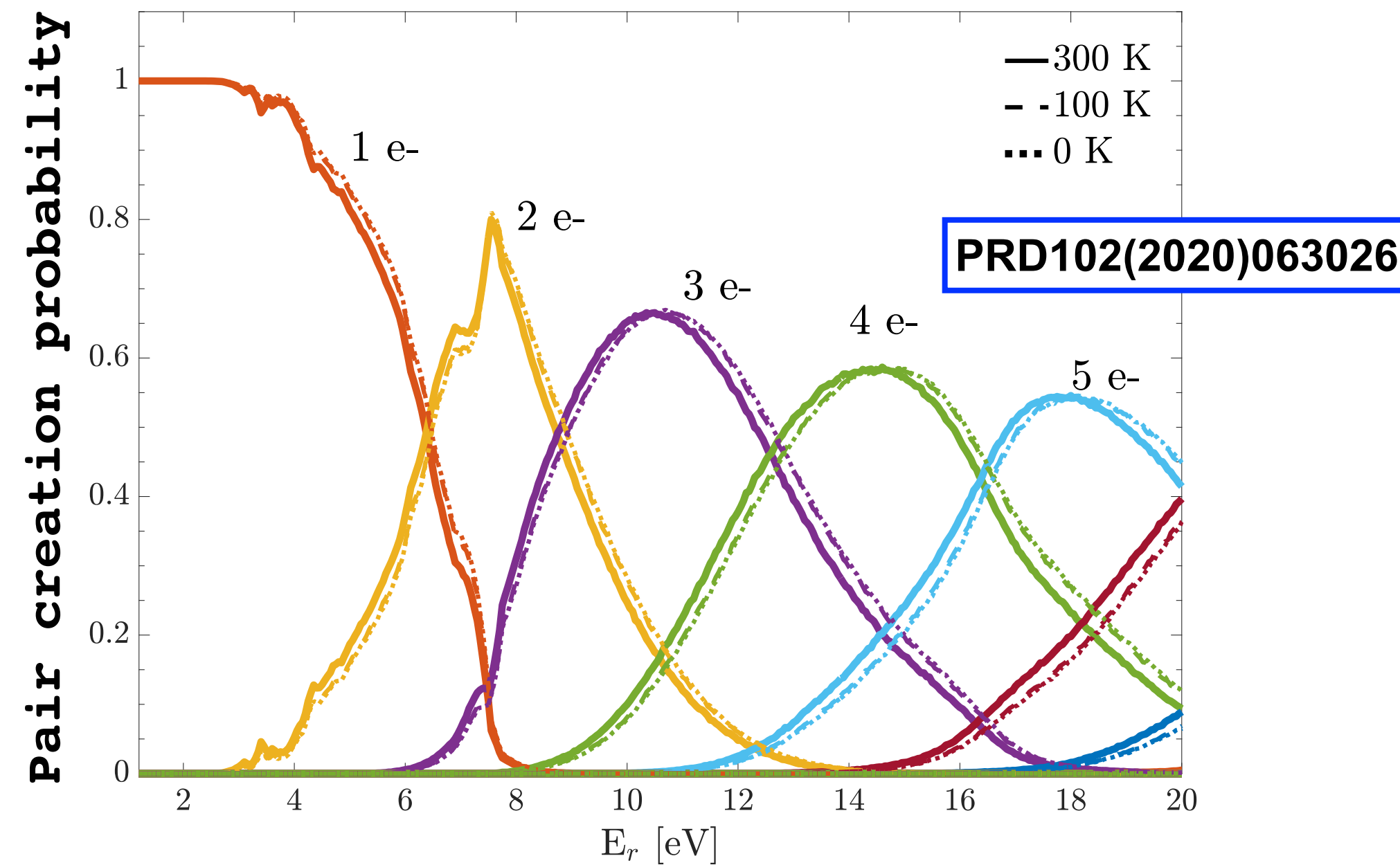
Electronic recoil result re-interpreted as limit on DM-N scattering (Migdal) or DM absorption

# Sensitivity projections



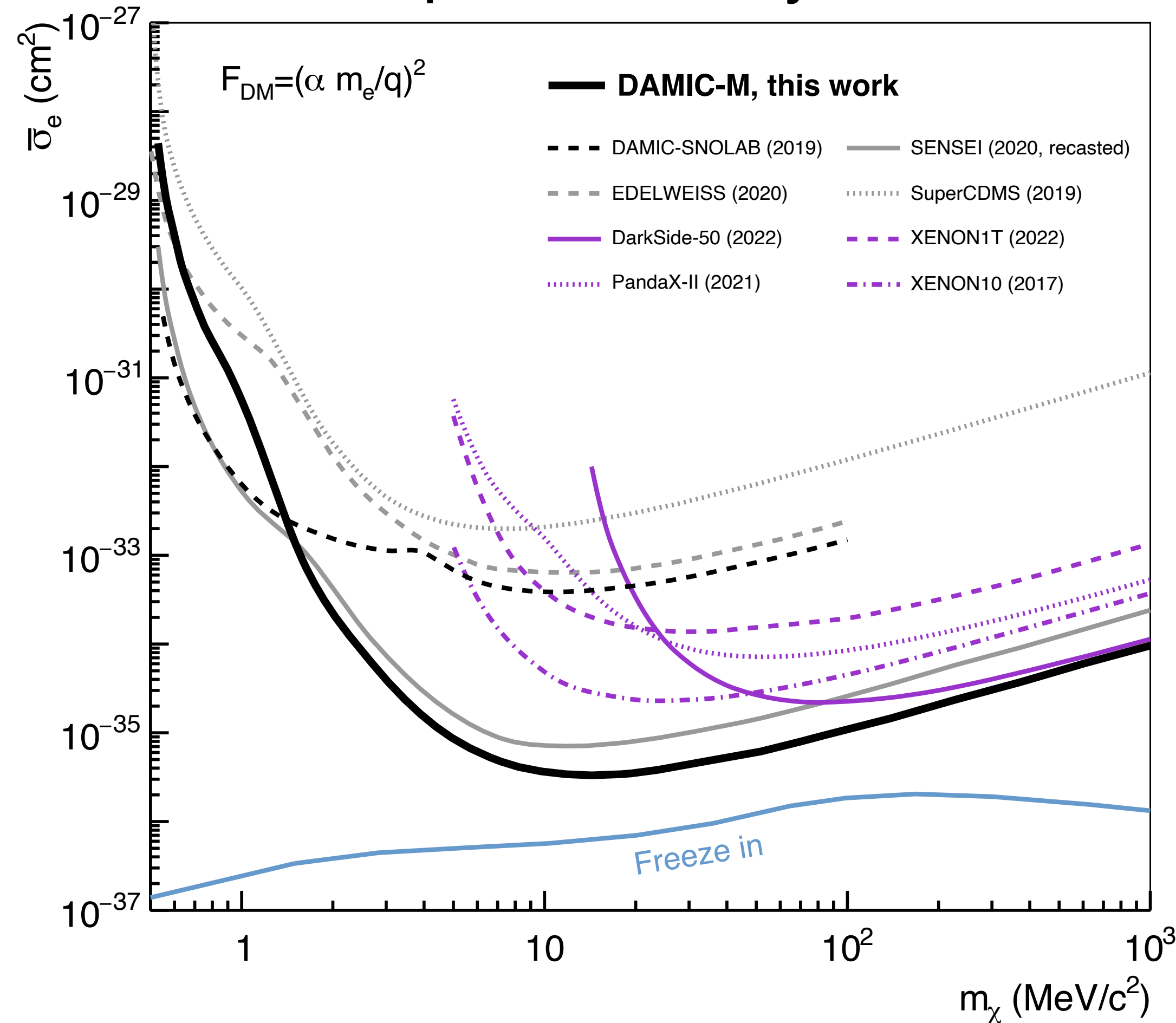
# CCD response

- Extensive research program to characterize the response of CCDs: energy / z recon.
- Sources: optical photons, X rays,  $\gamma$  rays, neutron sources, etc.
- Detailed models, e.g., charge generation, diffusion and collection.

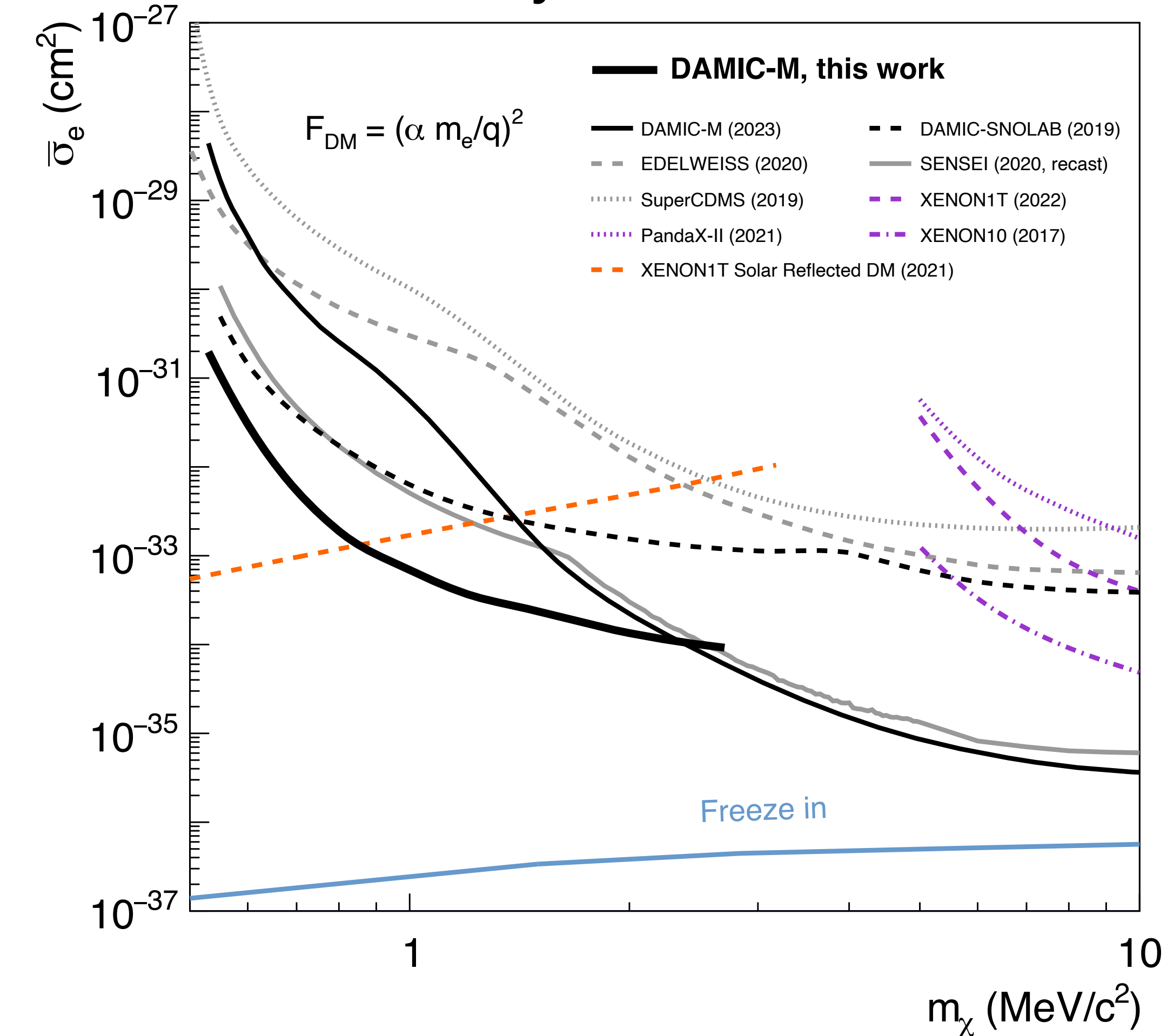


# SR1 results

## Spectral analysis



## Daily modulation



# Daily modulation

